DLR TAU Simulations for the Third AIAA Sonic Boom Prediction Workshop

Jochen Kirz

Ralf Rudnik

Institute of Aerodynamics and
Flow Technology
Braunschweig, Germany

DLR

Outline

- Summary of Cases Analyzed
- Flow Solver and Computing Platform
- Geometry Modifications and Grid Generation
- Results
  - Convergence
  - Biconvex
  - C608
- Summary and Outlook

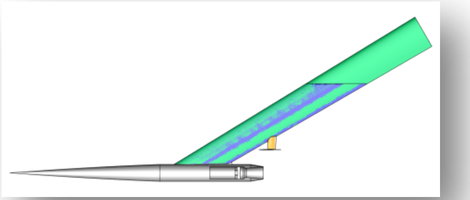

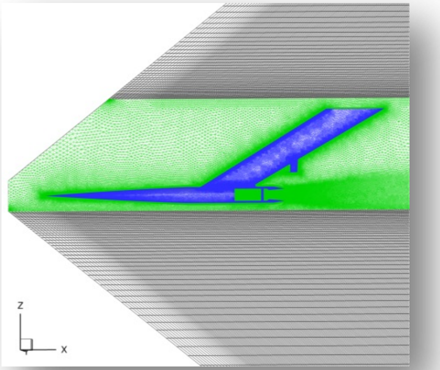

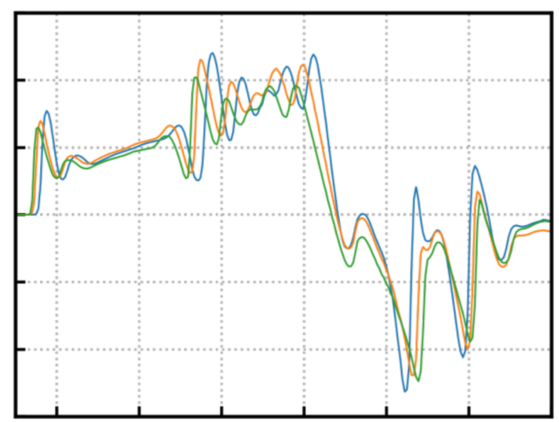

Summary of Cases Analyzed

NASA Biconvex 9×7 Shock-Plume Interaction Model

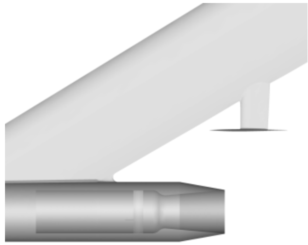

Workshop-provided	CENTAUR-generated
ws-mixed-157	centaur-mixed-100
ws-mixed-128	centaur-mixed-080
ws-mixed-100	centaur-mixed-100-nobico
ws-tet-157	centaur-mixed-100-clean
ws-tet-128	
ws-tet-100	centaur-euler-mixed-100

* Euler simulation / grid
* Minor geometry modifications
* Significant geometry modifications
* Original geometry, viscous simulation, submitted

NASA C608 Low Boom Flight Demonstrator

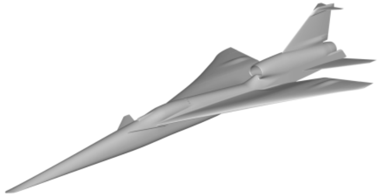

Workshop-provided	
ws-mixed-128	ws-tet-128
ws-mixed-100	ws-tet-100
ws-mixed-080	ws-tet-080
ws-mixed-064	ws-tet-064
ws-mixed-050	ws-tet-050
ws-mixed-040	

* Obtained after data submission deadline
* Original geometry, viscous simulation, submitted

Flow Solver and Computing Platform

DLR TAU Code Version 2018.1.0

- unstructured finite-volume
- hybrid grids
- Euler and RANS simulations (SA-negative turbulence model)
- 2nd order Upwind scheme (AUSMDV) with SRR limiter
- backward Euler (LU-SGS) time stepping
- no multigrid acceleration
- Green-Gauss reconstruction of gradients

$C^2A^2S^2E^2$ Cluster [shut down in Dec 2019]

- parallel
- distributed memory
- 1 computing node (24 cores) per 250.000 grid nodes (max 8 nodes)
- run time 1-8h depending on grid refinement

CARA Cluster [since Dec 2019]

- parallel
- distributed memory
- 1 computing node (64 cores) per 300.000 grid nodes (max 10 nodes)
- run time 0.5-2h

Geometry Modifications
Biconvex

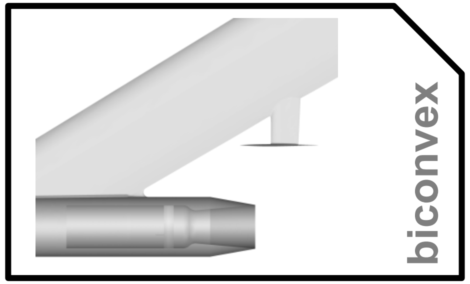

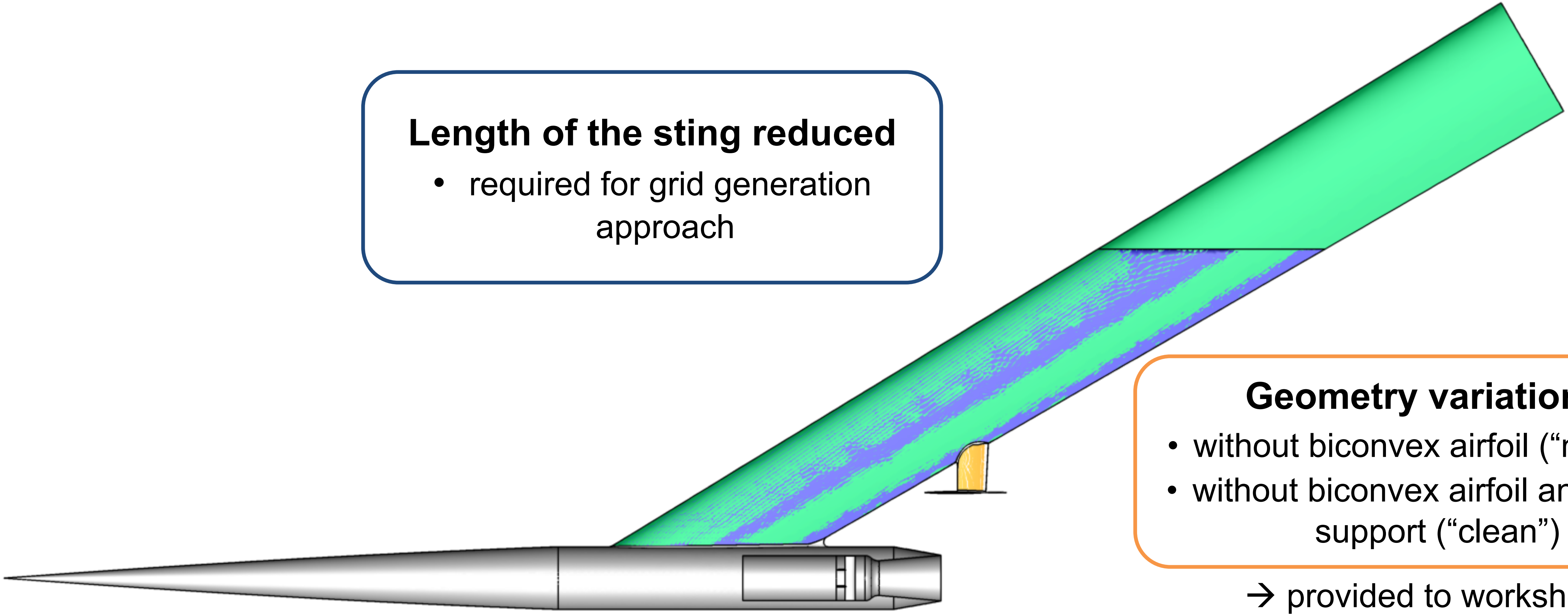

Length of the sting reduced

- required for grid generation approach

Geometry variations

- without biconvex airfoil (“nobico”)
- without biconvex airfoil and airfoil support (“clean”)

→ provided to workshop as optional grids

Grid Generation

Biconvex – Grid Generation Method using CENTAUR

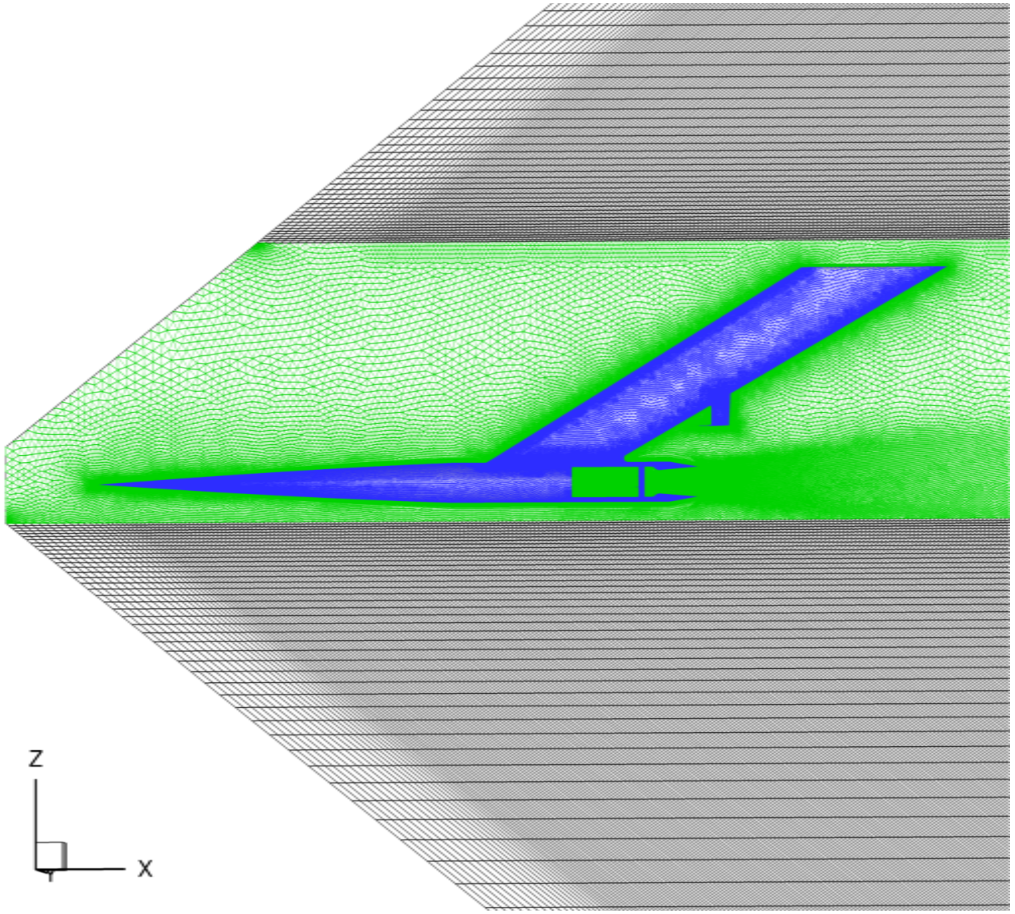

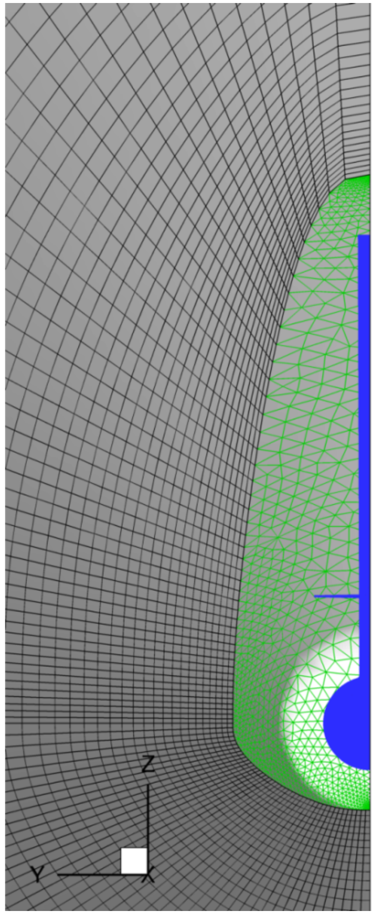

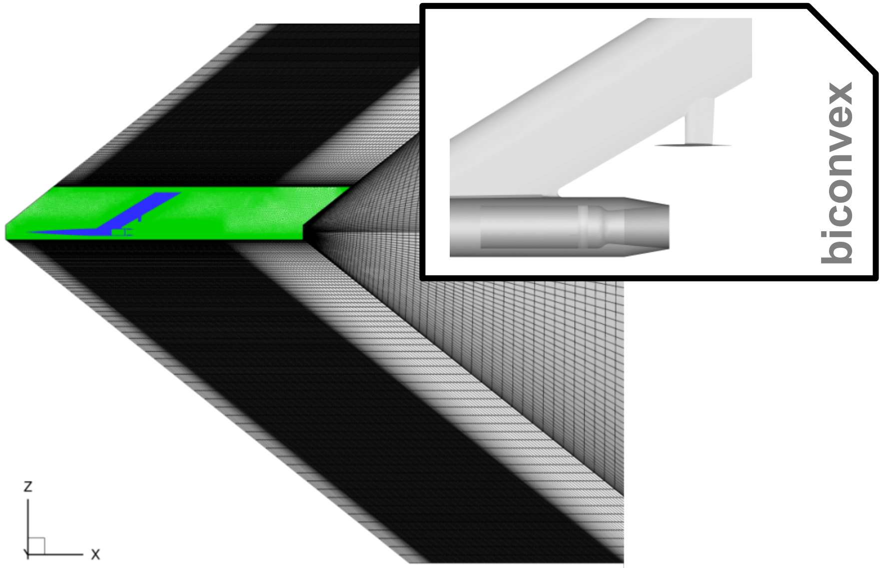

Grid Generation Approach using CENTAUR

- unstructured hybrid grids
- prisms for boundary layer resolution
- tetrahedra in mid-field
- structured far-field (Mach cone aligned)

Far-field Setup

- 3.5mm cell size at interface to mid-field
- 1.05 stretching in radial direction
- $R_{max}/L \approx 3$
- 2° resolution in circumferential direction (coarser above geometry)

Grid Generation

Biconvex – Comparison of CENTAUR to Workshop-Provided Grids

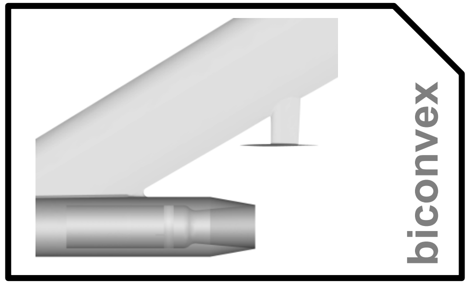

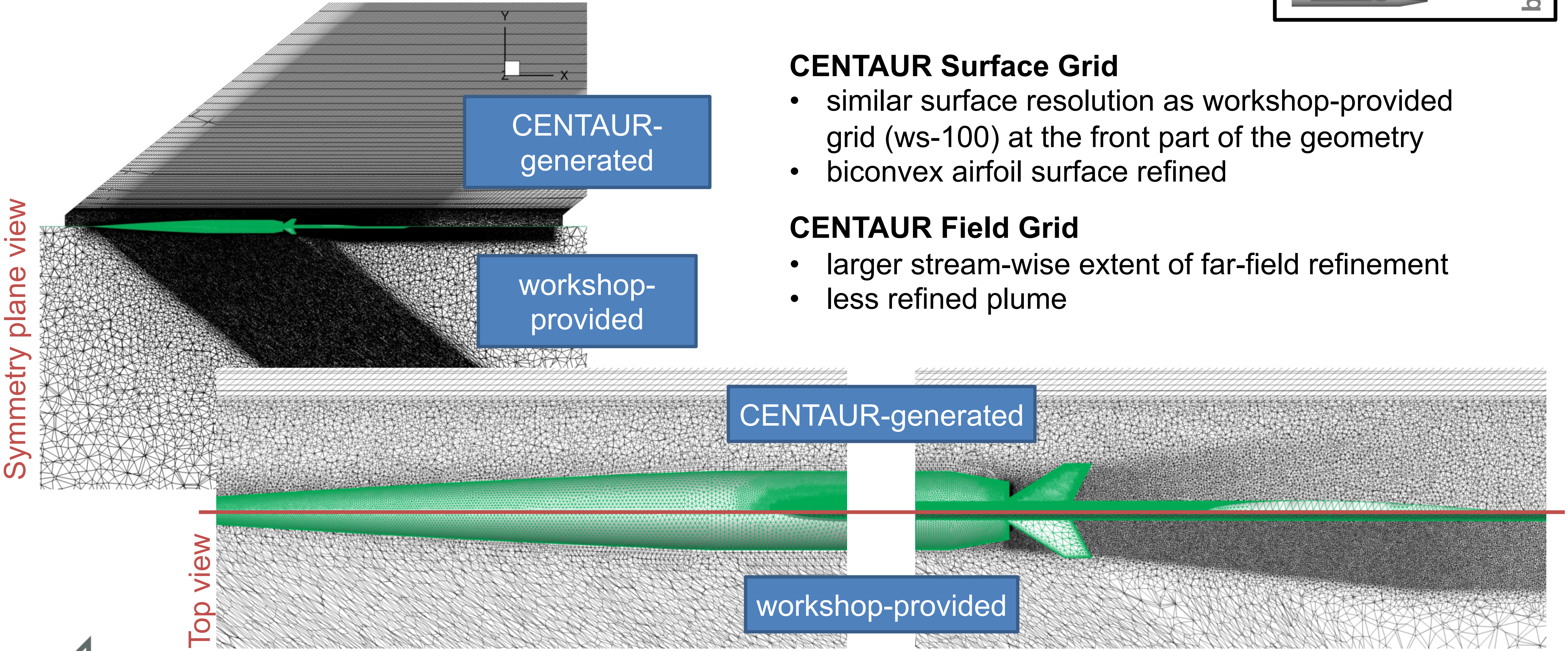

CENTAUR Surface Grid

- similar surface resolution as workshop-provided grid (ws-100) at the front part of the geometry
- biconvex airfoil surface refined

CENTAUR Field Grid

- larger stream-wise extent of far-field refinement
- less refined plume

Grid Generation
Biconvex – Comparison to Workshop-Provided Grids

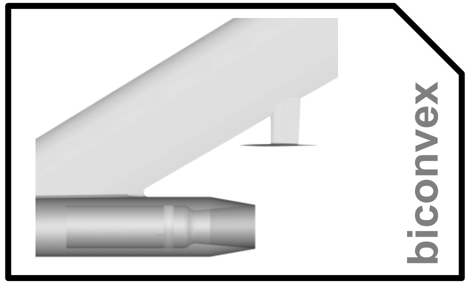

Grid	Nodes	Tetra	Prism	Hexa
centaur-100	8,883,678	8,872,591	9,649,628	2,174,670
centaur-080	14,252,283	12,898,047	14,266,887	4,421,034
centaur-100-nobico	7,776,110	7,542,565	7,517,414	2,378,705
centaur-100-clean	7,113,551	6,836,461	6,512,115	2,378,705
centaur-100-euler	4,278,382	10,619,339	0	2,174,670
ws-mixed-100	3,286,221	14,627,534	1,388,470	0
ws-tet-100	3,286,221	18,815,990	0	0

centaur-100, centaur-080: original geometry (shortened sting)

centaur-100-nobico, centaur-100-clean: modified geometry

centaur-100-euler: no prisms in boundary layer

Outline

- Summary of Cases Analyzed
- Flow Solver and Computing Platform
- Geometry Modifications and Grid Generation
- Results
  - Convergence
  - Biconvex
  - C608
- Summary and Outlook

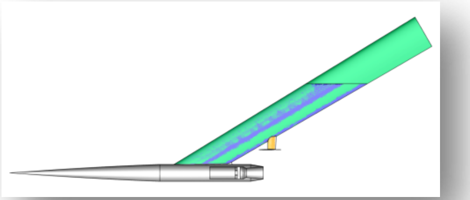

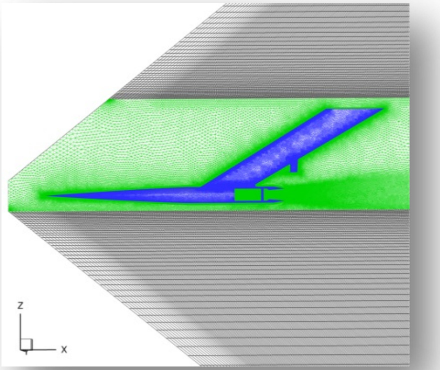

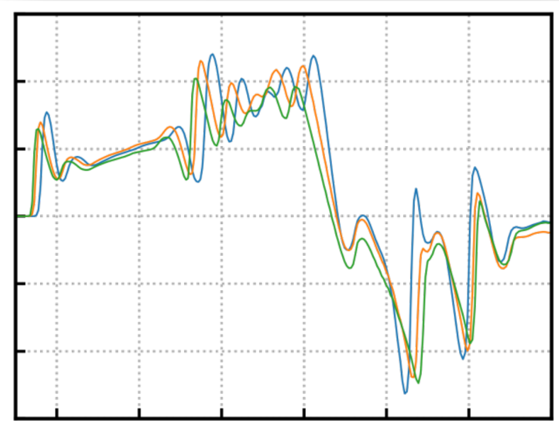

Results
Typical Convergence History

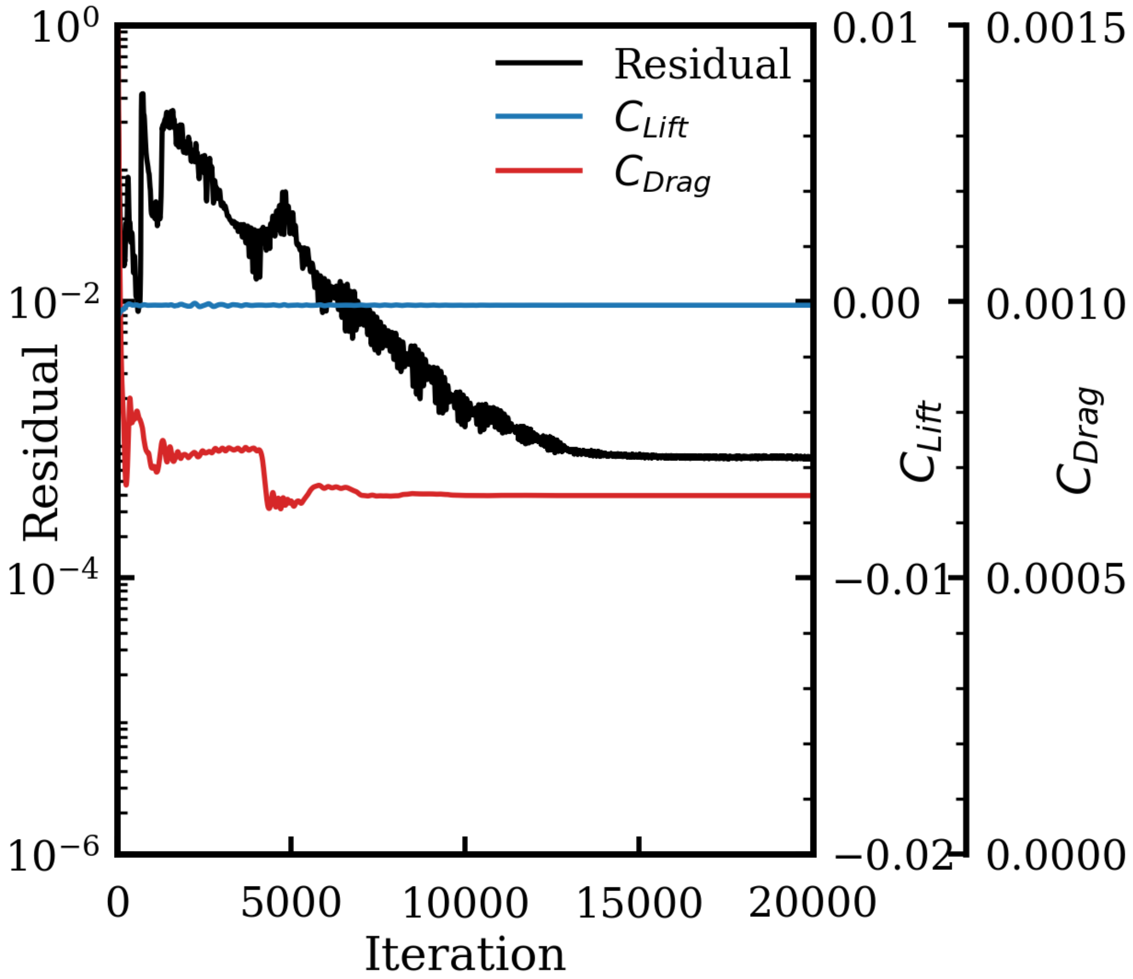

Startup Process
- started with M=1.1
- Mach number increased in steps of M=0.1 during simulation
- CFL number increased for faster convergence

Final Convergence
- 5000-10000 iterations to ensure information propagation of pressure disturbances to multiple body lengths distance

Results
Biconvex

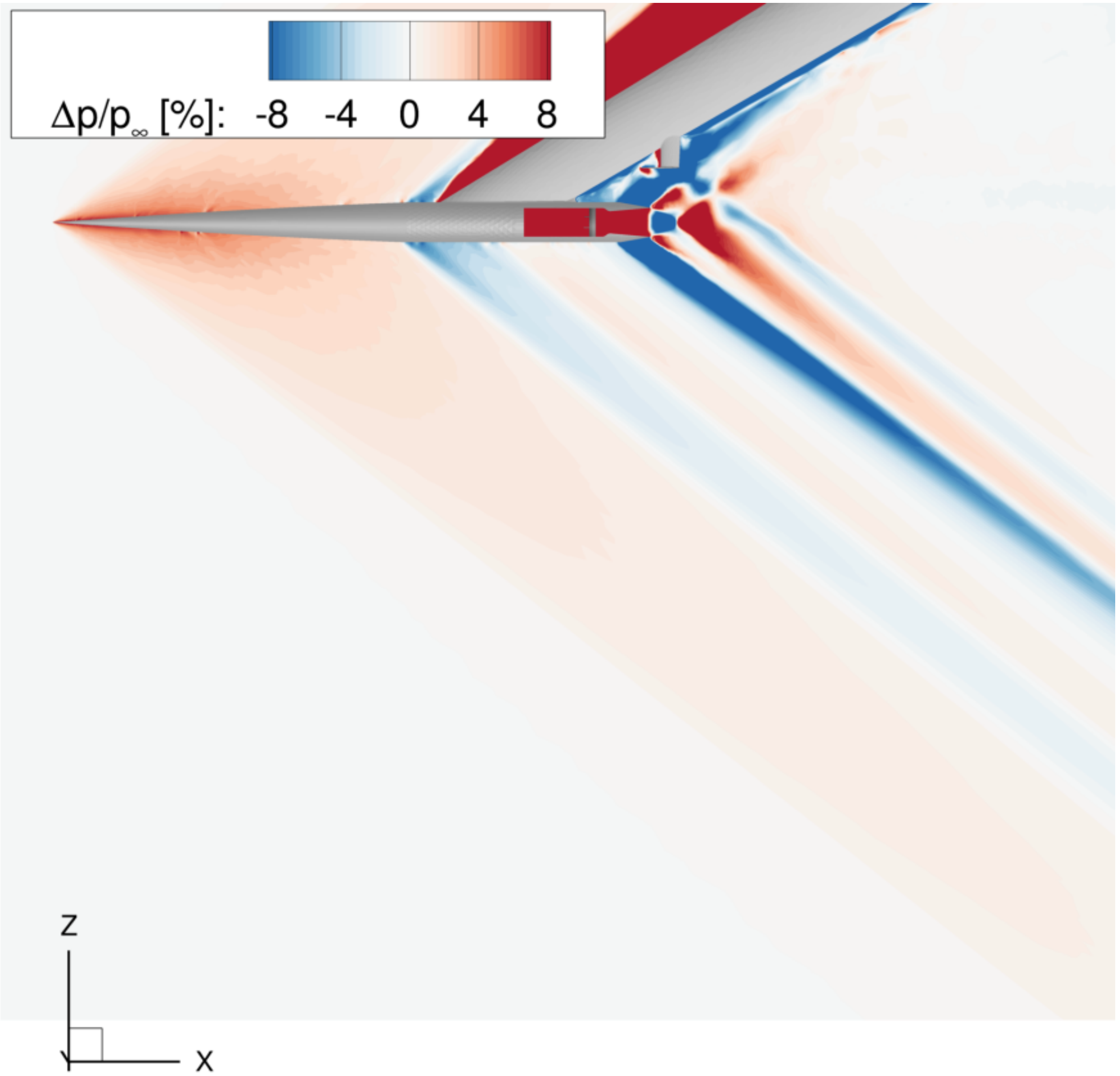

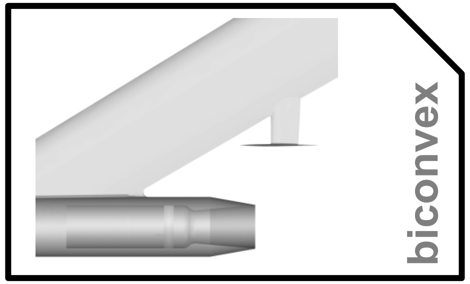

Workflow

Results
Biconvex

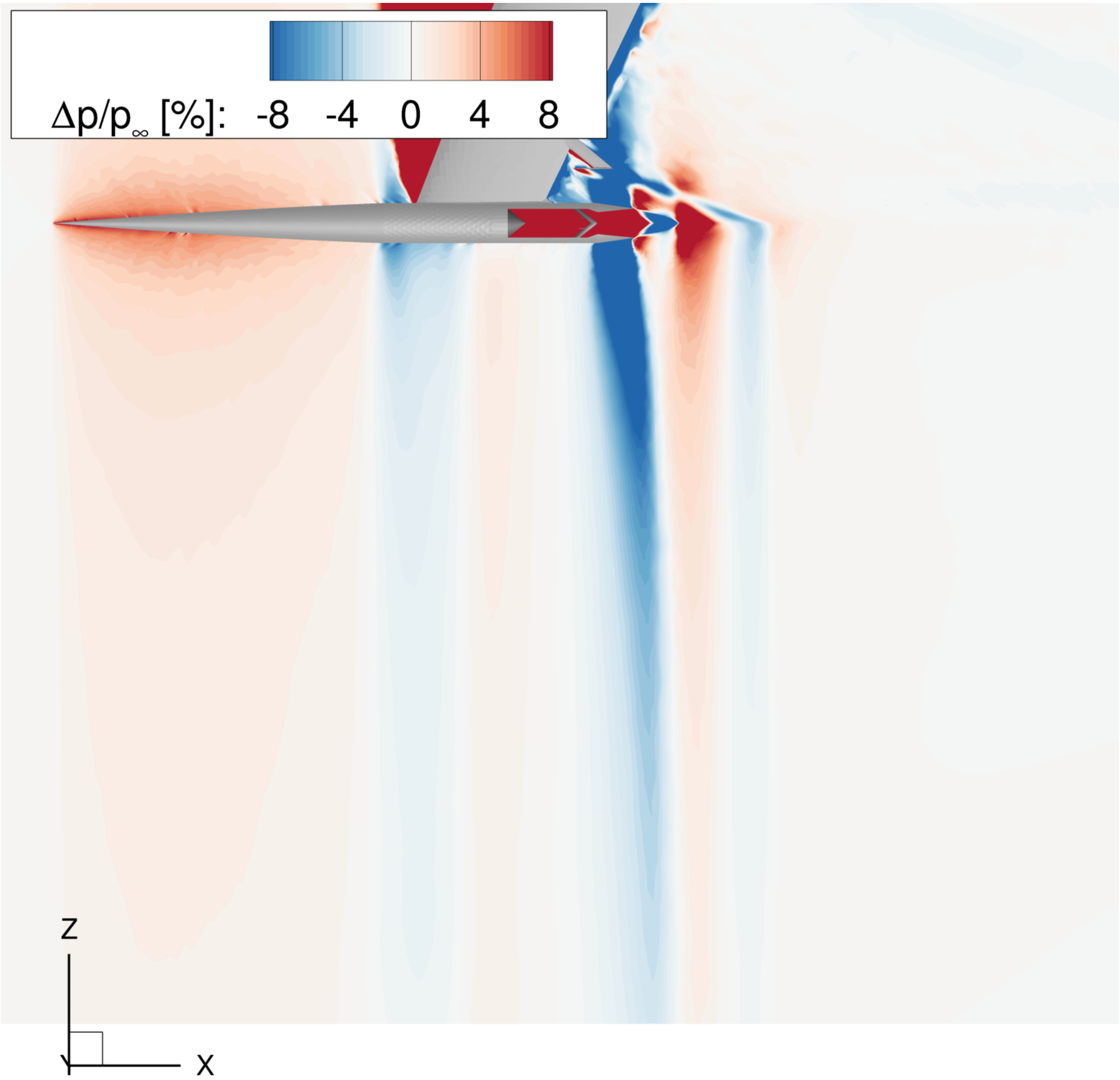

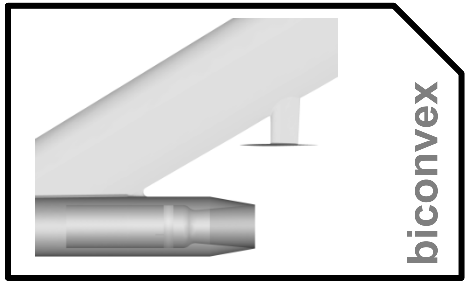

Workflow

Step 1

- align x coordinate to Mach cone

Results
Biconvex

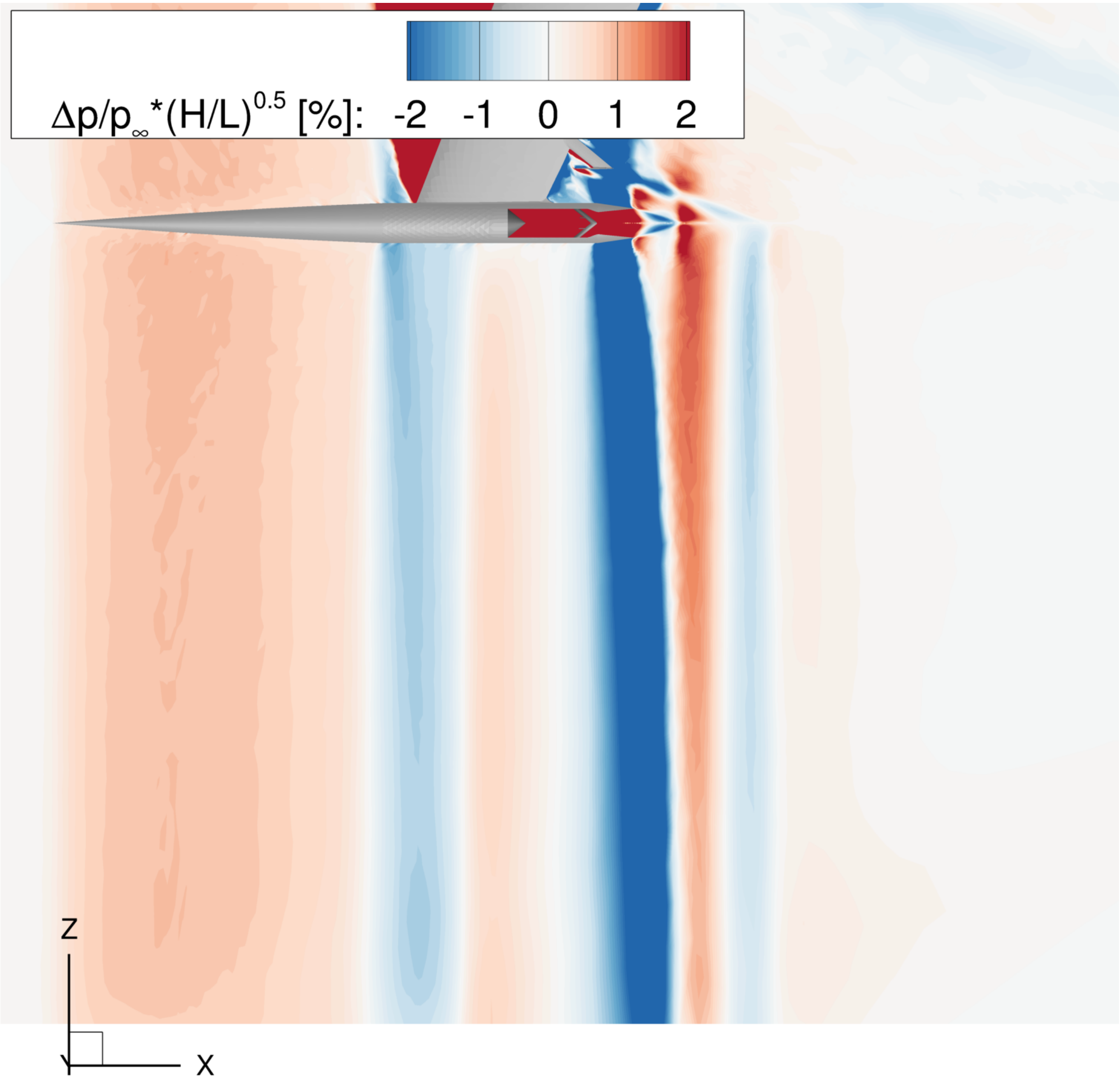

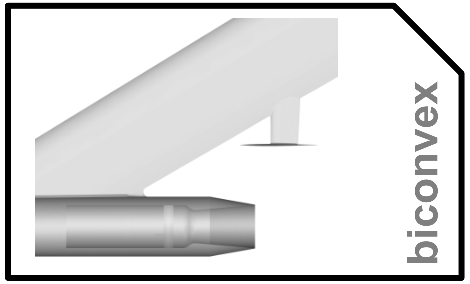

Workflow

Step 1

- align x coordinate to Mach cone

Step 2

- normalize pressure with the square root of the extraction distance

Results
Biconvex

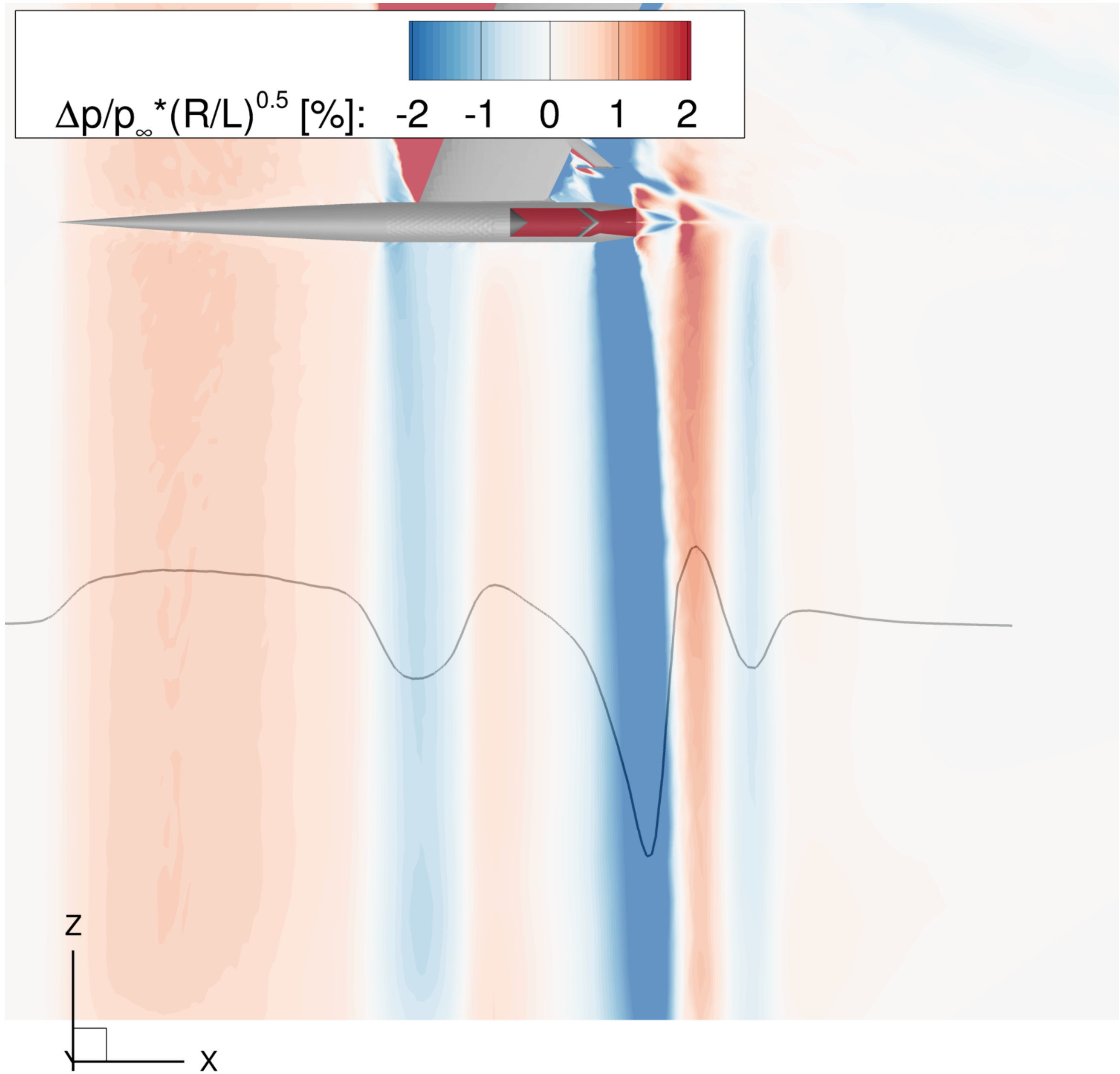

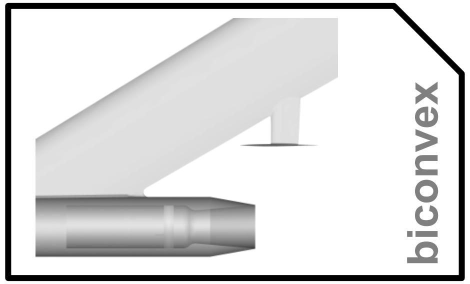

Workflow

Step 1
- align x coordinate to Mach cone

Step 2
- normalize pressure with the square root of the extraction distance

Step 3
- extract pressure signatures with normalized x coordinates and pressure values

Results
Biconvex

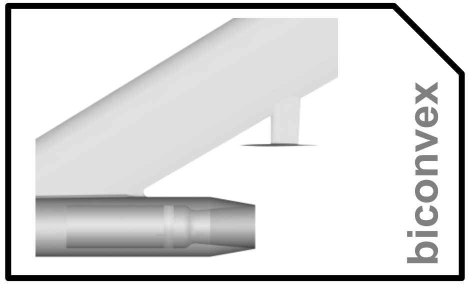

centaur-mixed-100-clean

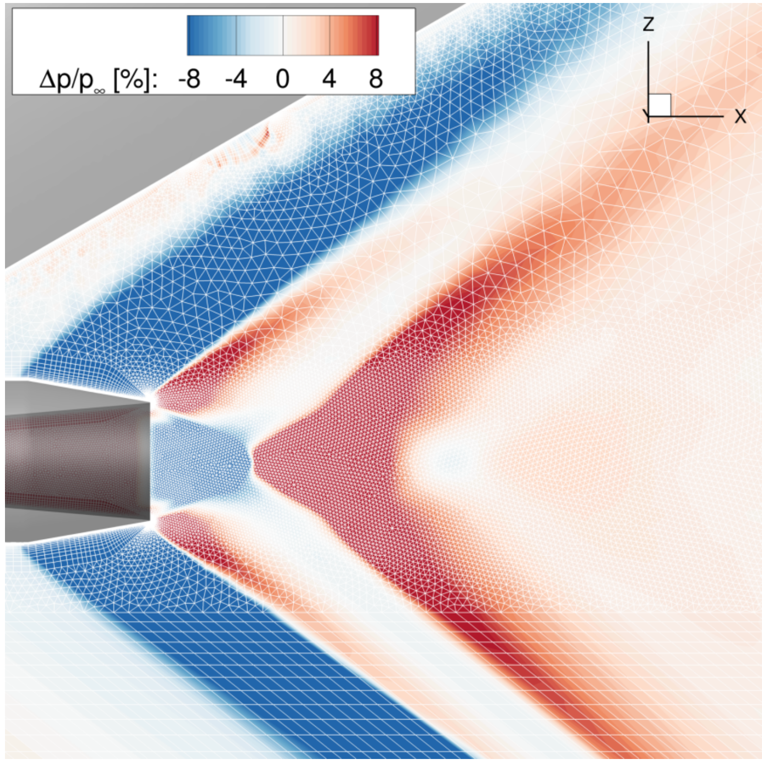

centaur-mixed-100-nobico

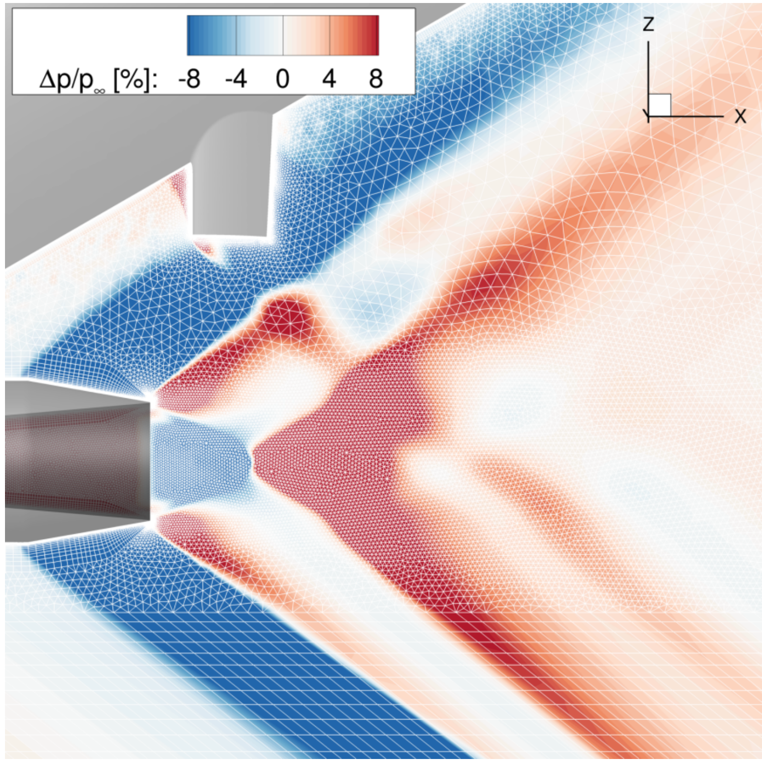

centaur-mixed-100

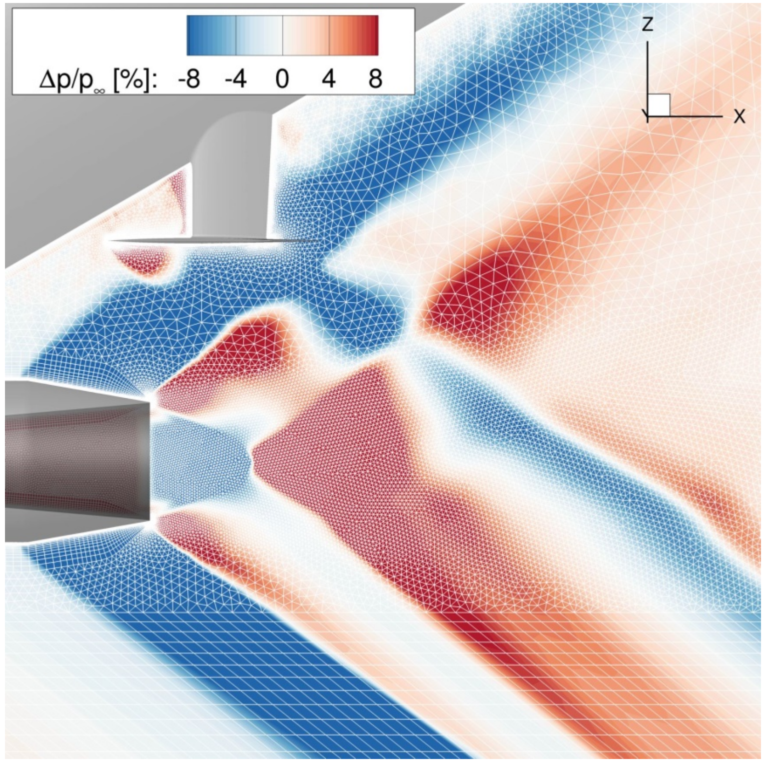

Results
Biconvex

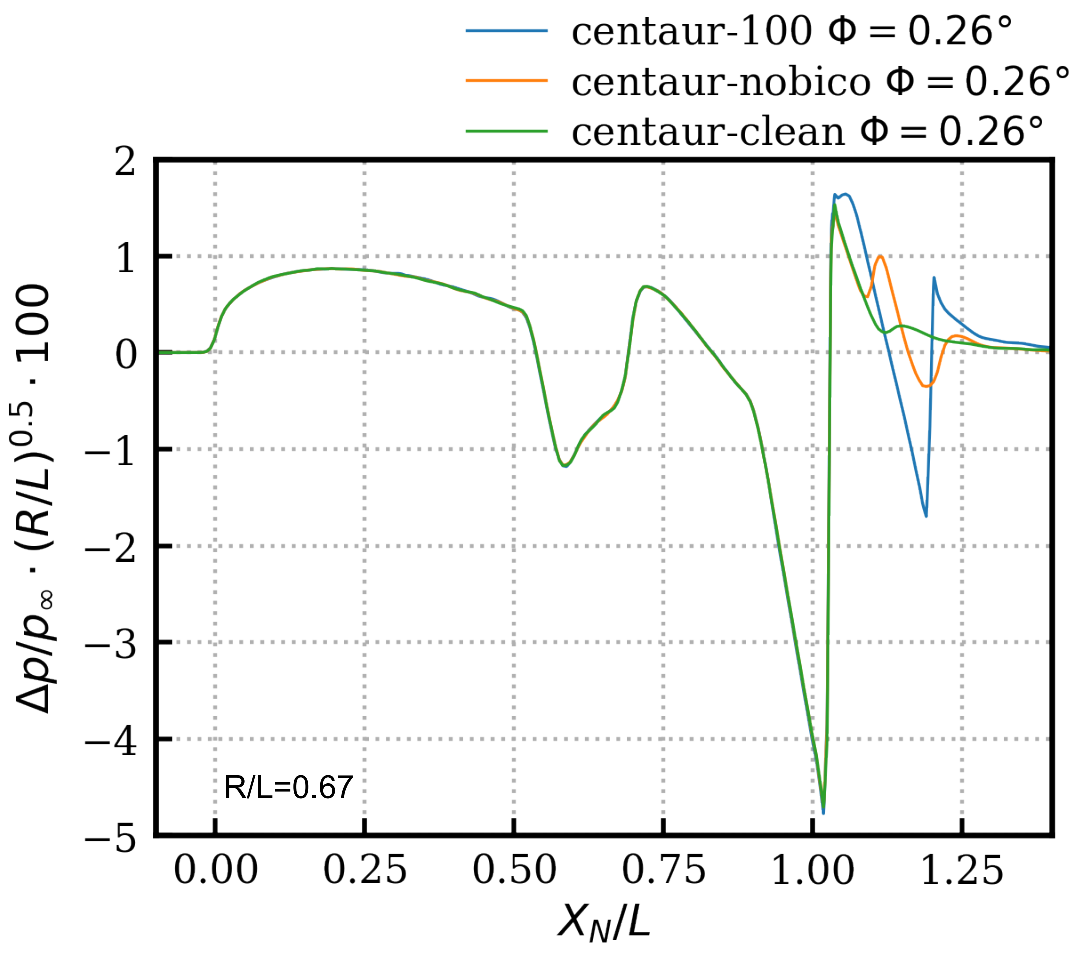

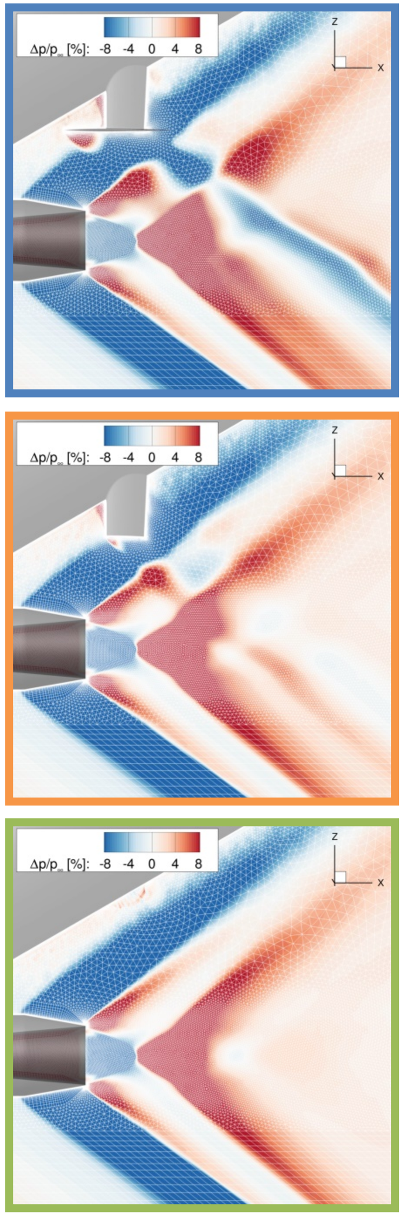

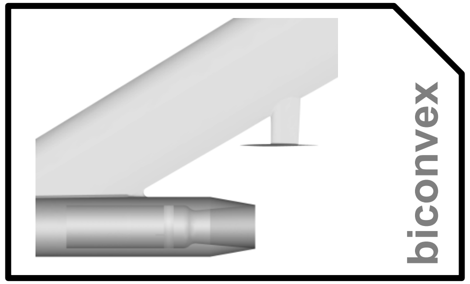

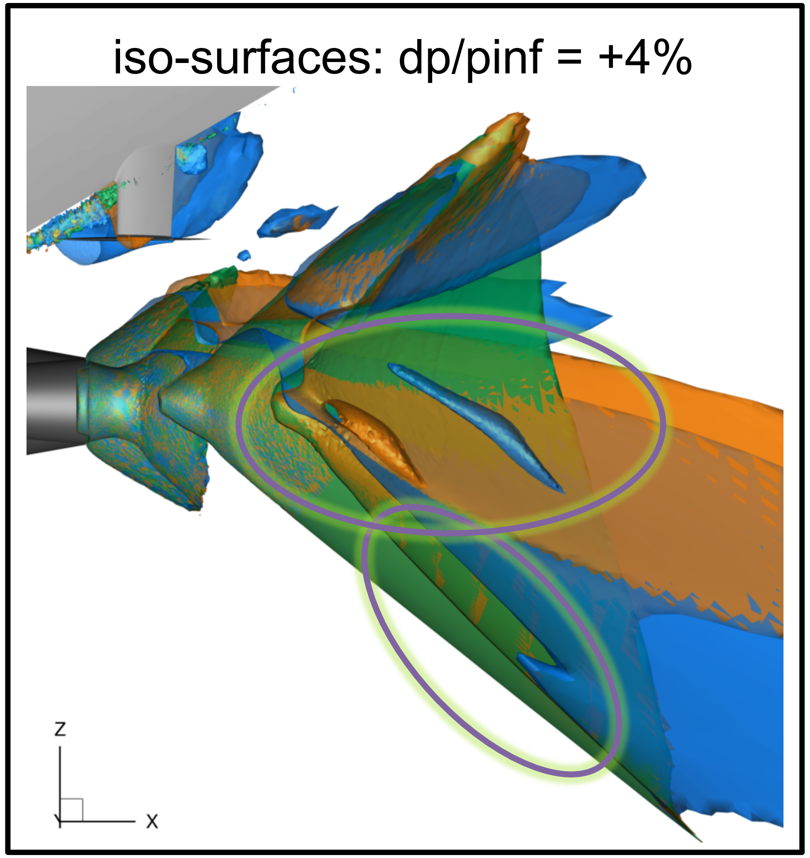

Results

Biconvex – CENTAUR-Generated vs Workshop-Provided Grids

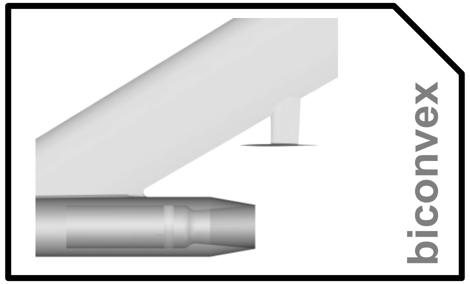

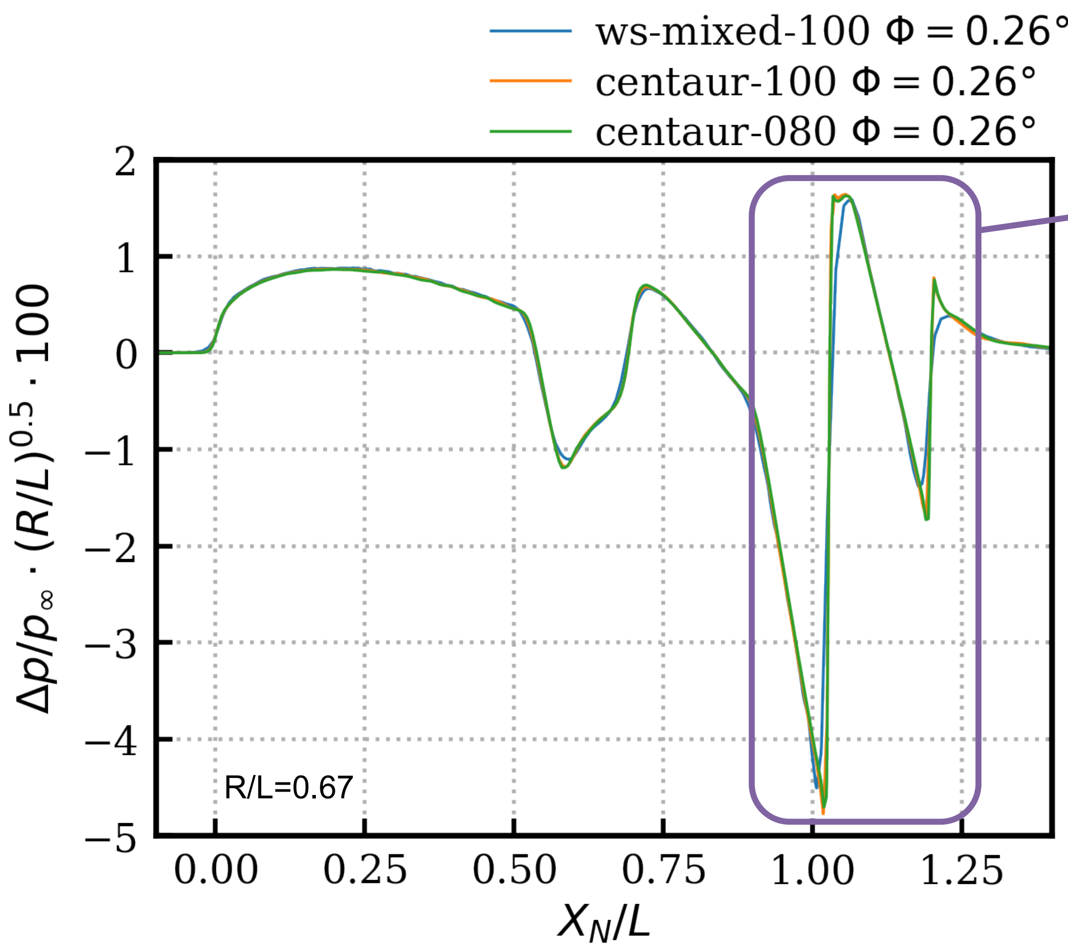

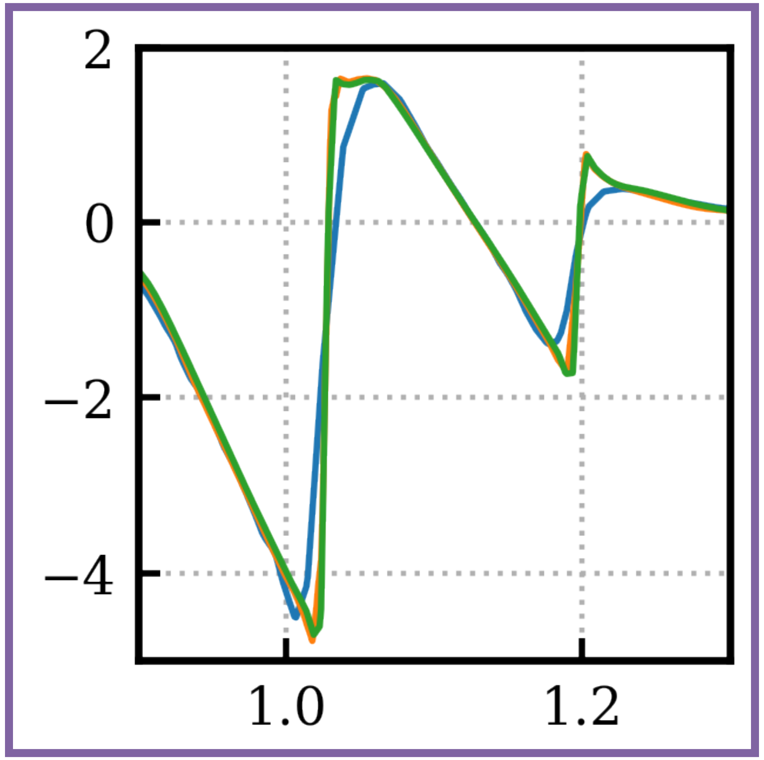

Better resolution of the interaction using the CENTAUR grids

→ interaction of leading edge shock of biconvex airfoil and plume shock better resolved (no complete coalescence)

Minor difference between the grid refinement levels of the CENTAUR grids

→grid convergence achieved

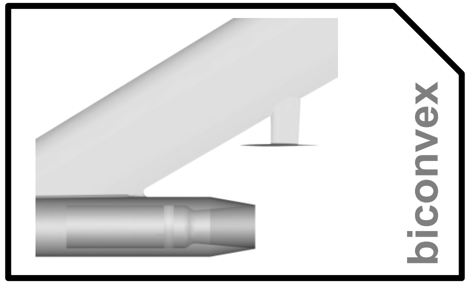

Results

Biconvex – Coarse Workshop Grid (ws-mixed-157)

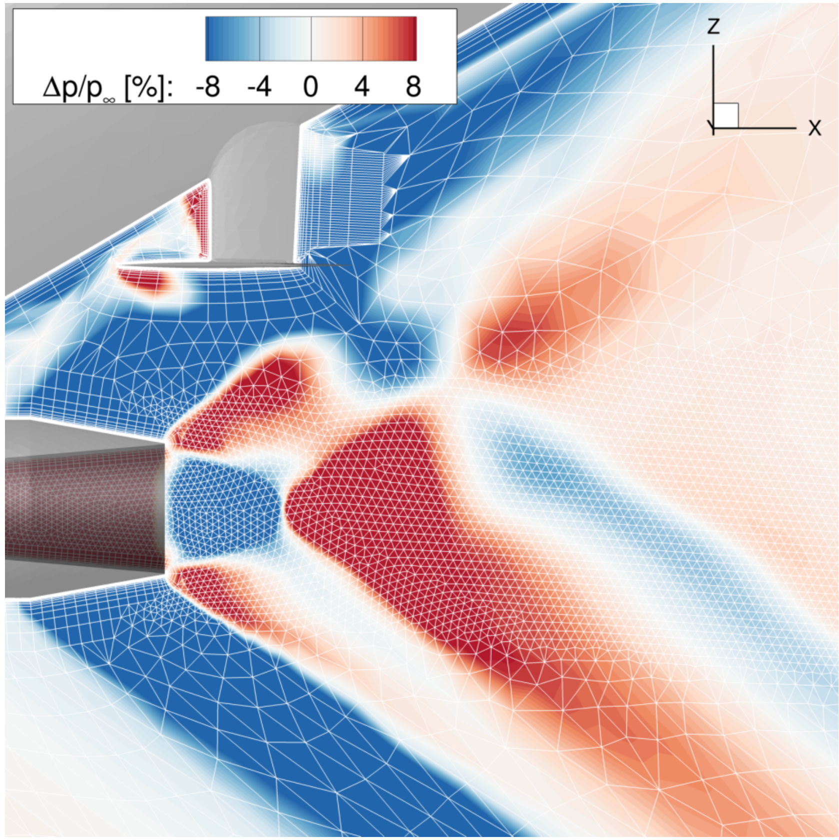

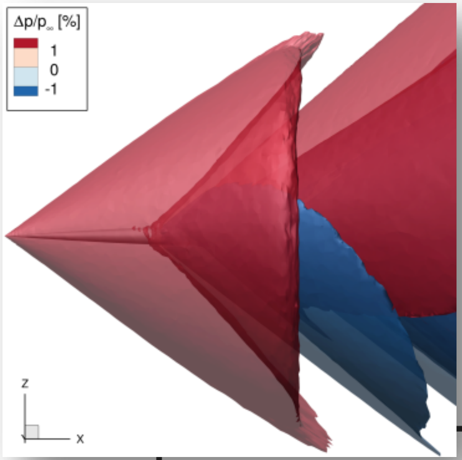

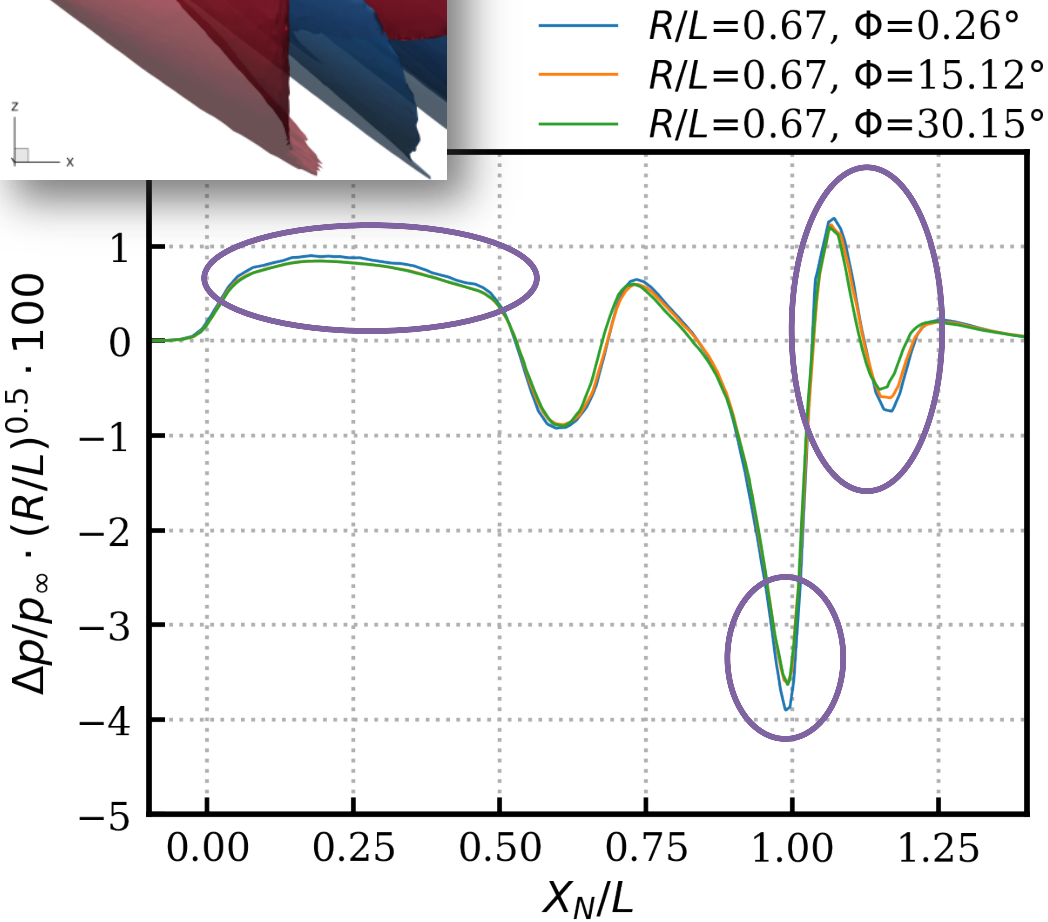

- non axi-symmetric pressure signature at the nose
- larger magnitude of shocks and expansions on-track in interaction region

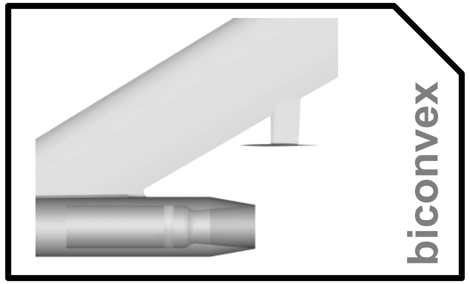

Results

Biconvex – Fine Workshop Grid (ws-mixed-100)

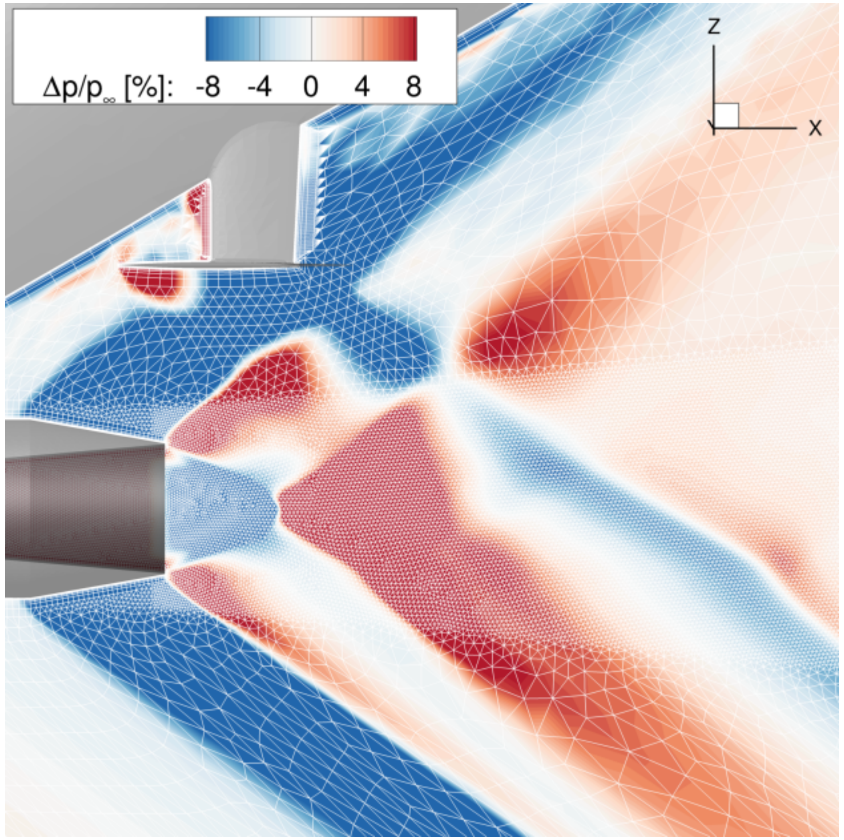

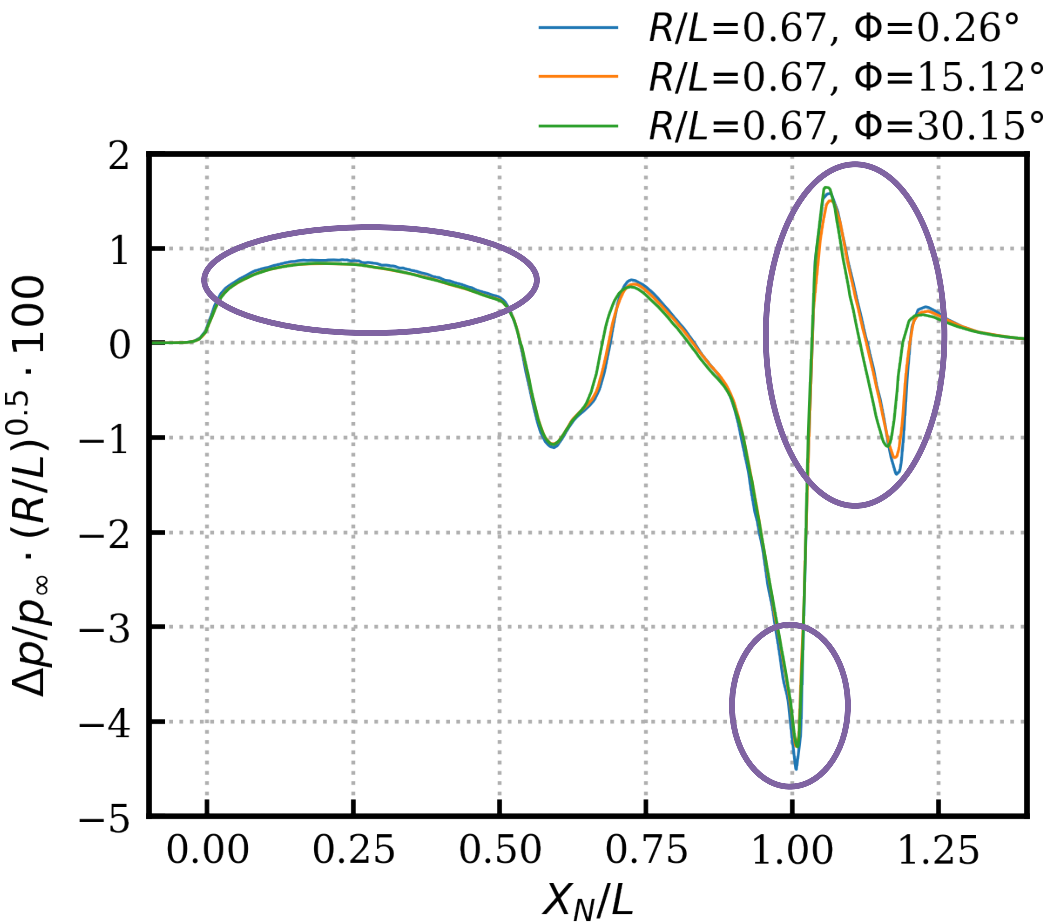

- pressure field at the nose is more axisymmetric
- larger magnitude of shocks and expansions on-track in interaction region

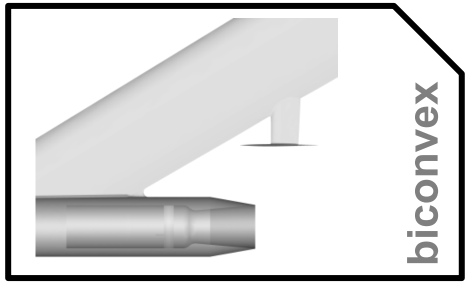

Results

Biconvex – Signature convergence with grid refinement (on-track)

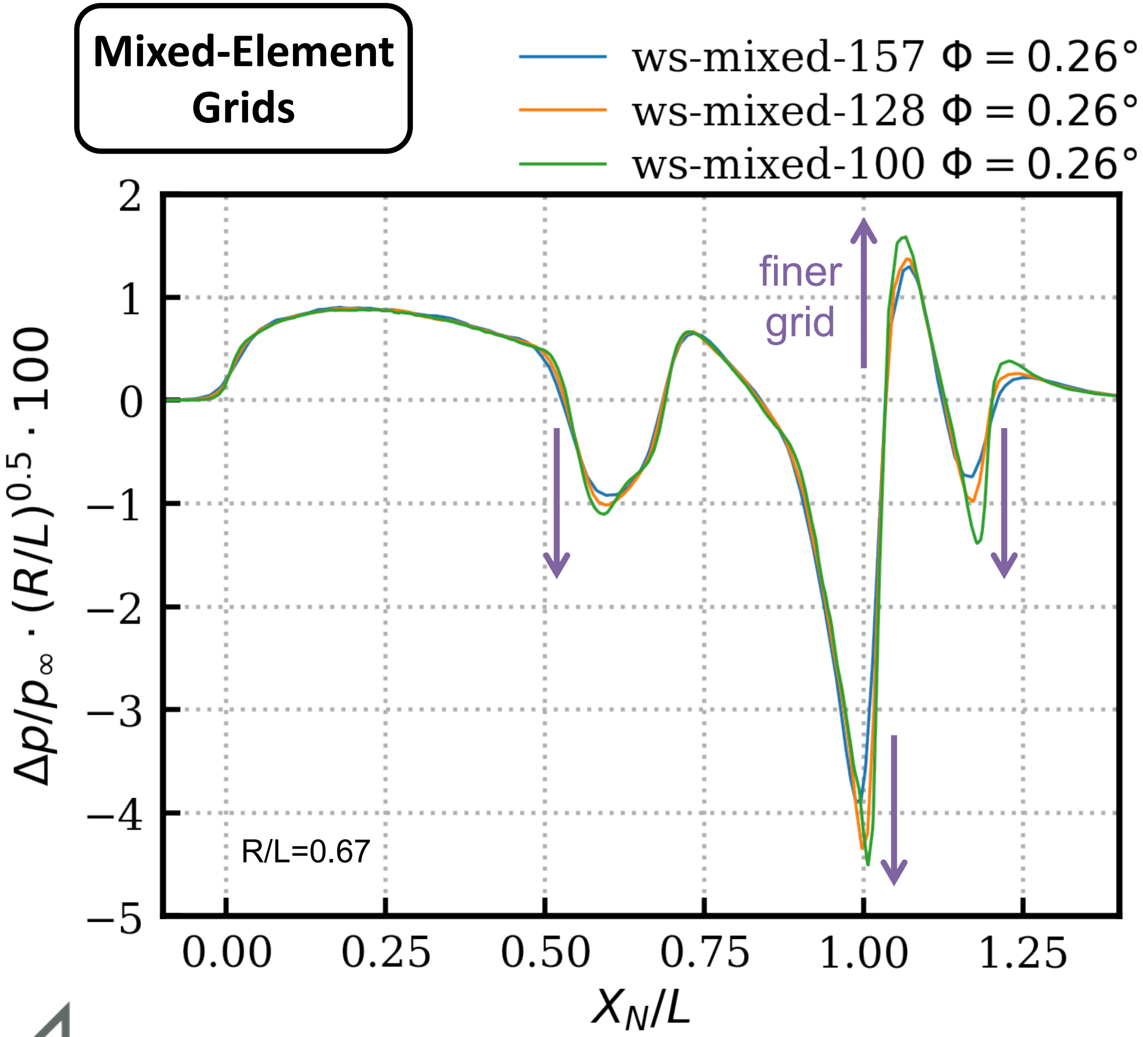

- larger magnitude of shocks and expansions for finer grids
  → less numerical dissipation
  → already observed for SBPW1 and SBPW2 cases
- no pressure signature convergence achieved for workshop-provided grids

Results

Biconvex – Signature convergence with grid refinement (on-track)

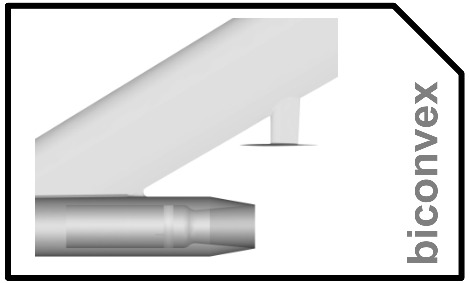

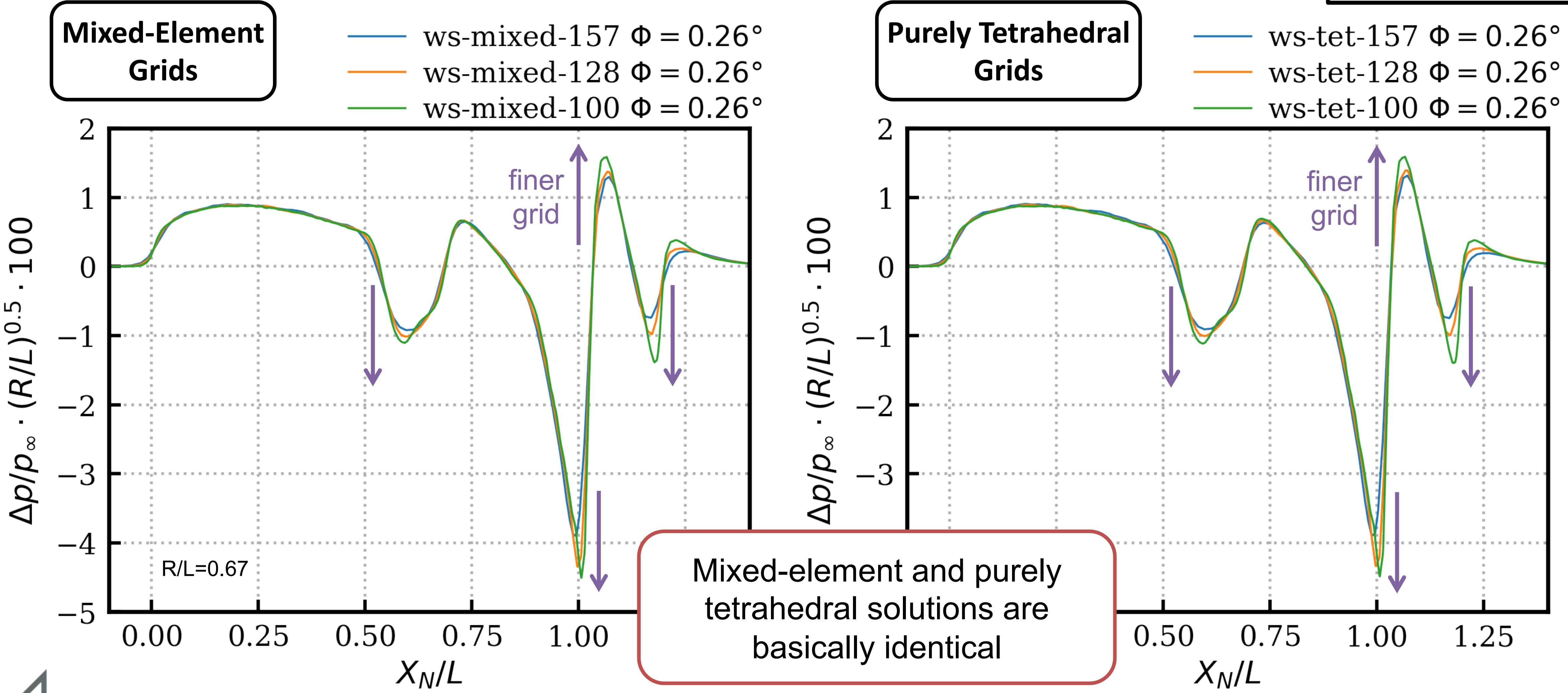

Mixed-element and purely tetrahedral solutions are basically identical

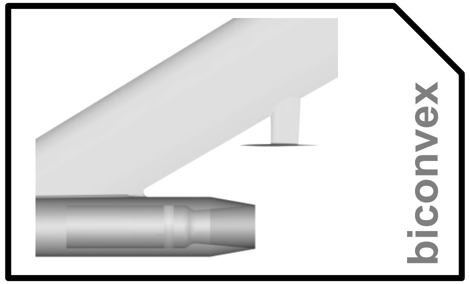

Results

Biconvex – Comparison of RANS and Euler Simulations

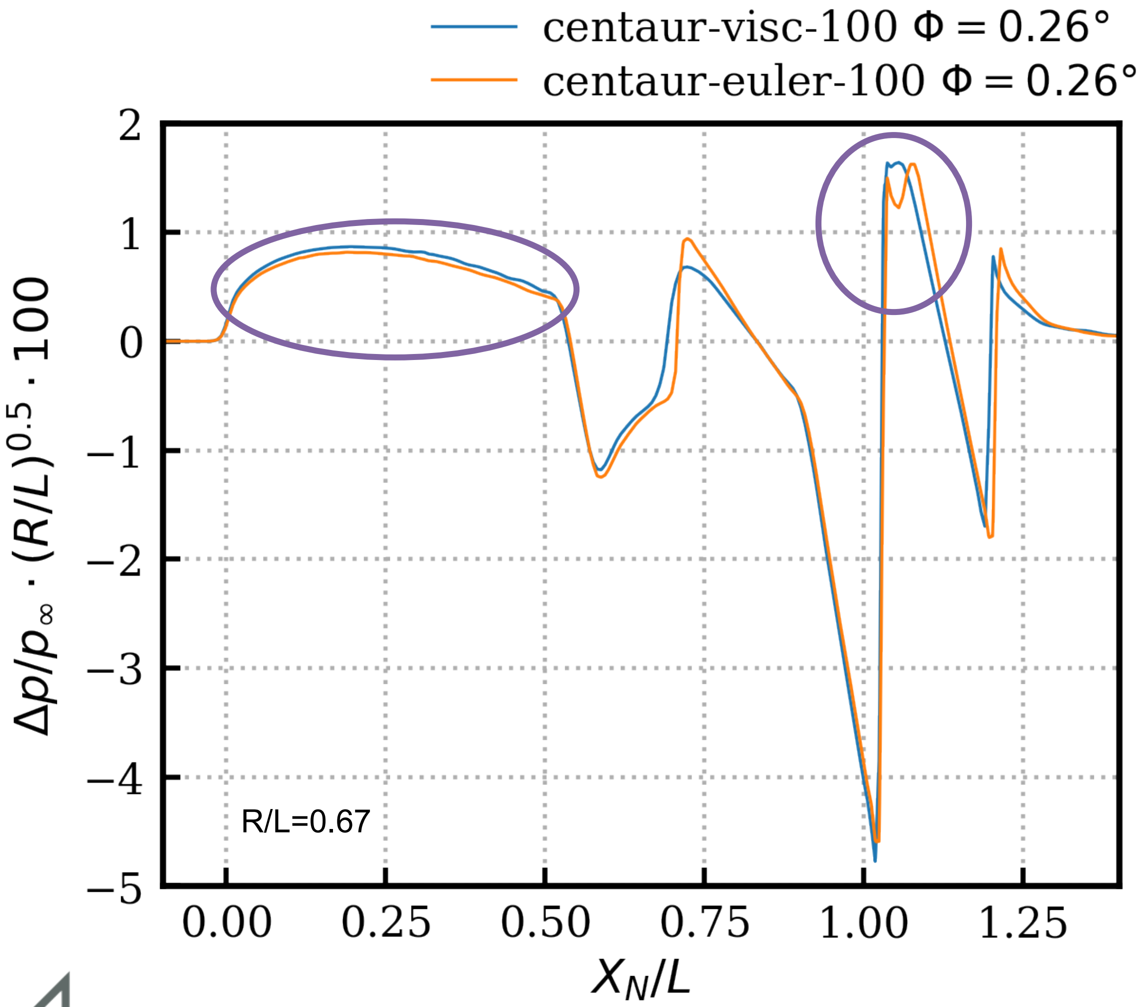

- front part of the pressure signature influenced by boundary layer
  - effective thickening of the body due to the boundary layer
  - NOT a consequence of surface resolution near the symmetry plane
- less coalescence of the plume shock and the leading edge shock of the biconvex airfoil for Euler simulations

Results
C608

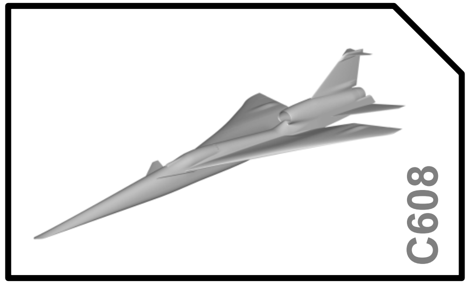

Strong compression at the nose with following expansion

Canard interacting with expansion due to fuselage shape

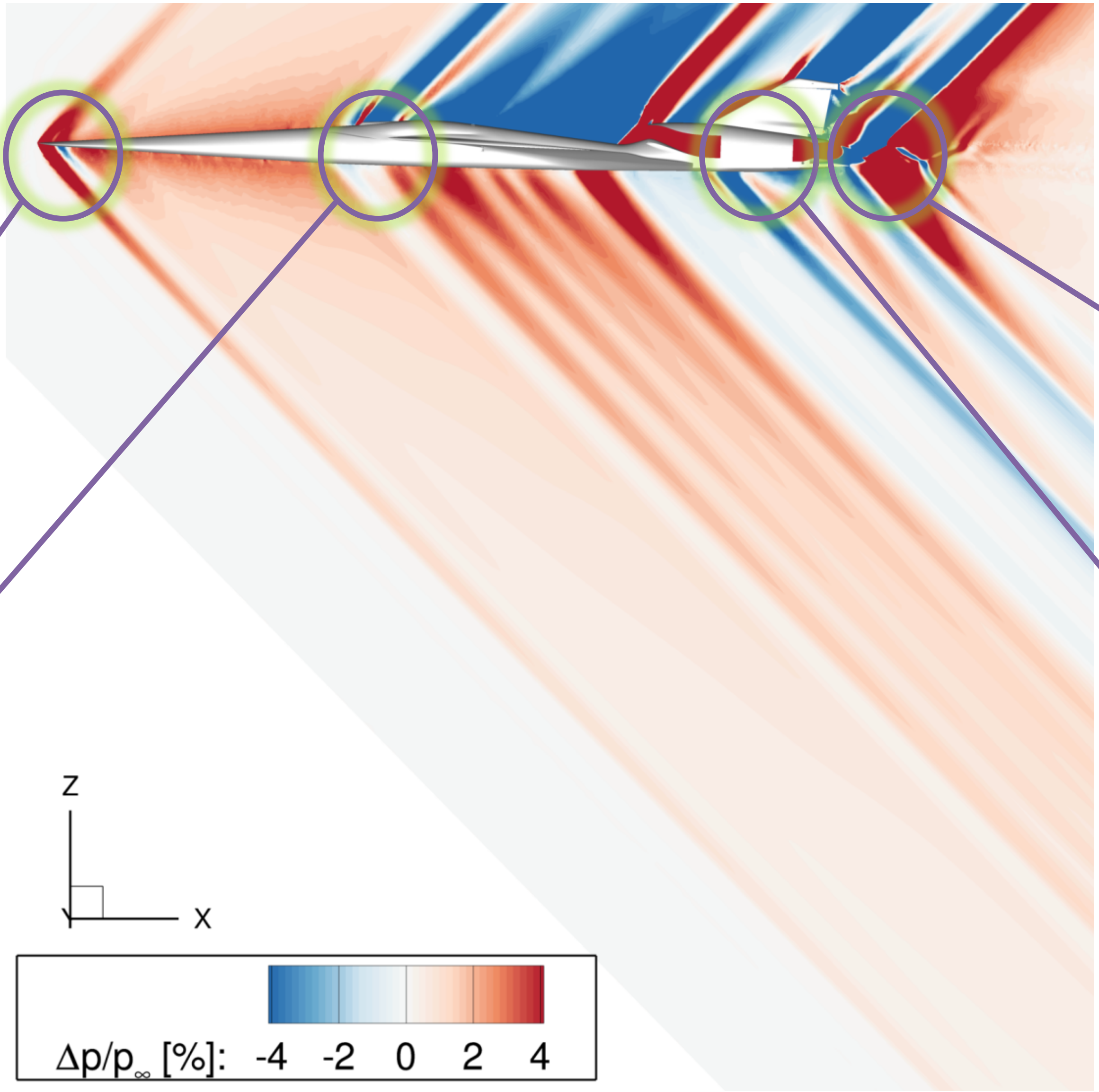

grid: ws-mixed-100

Shock-plume interations

HTP interacting with expansion due to fuselage shape

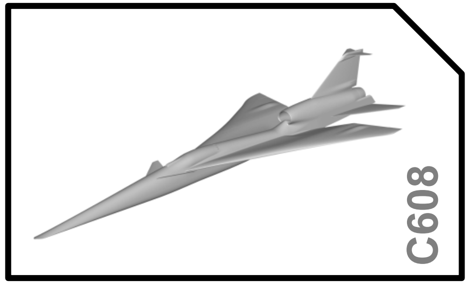

Results
C608 – Signature Propagation

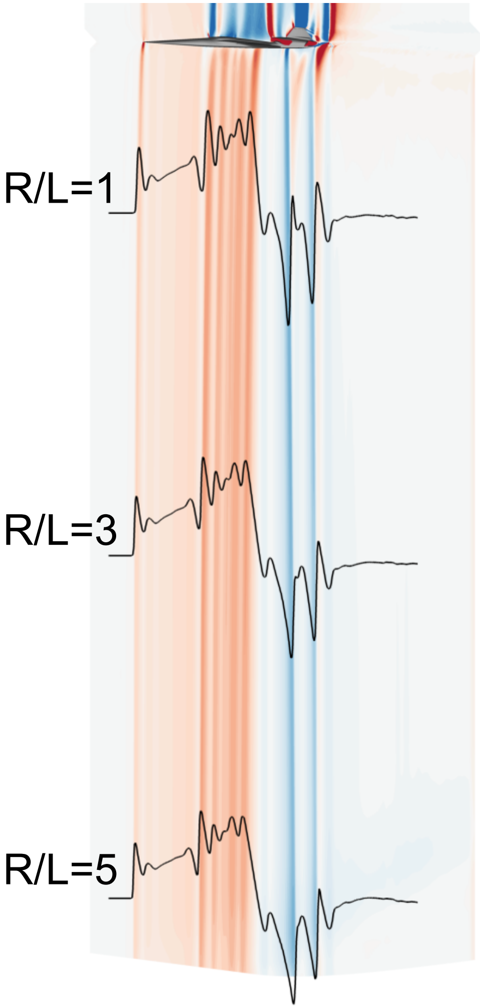

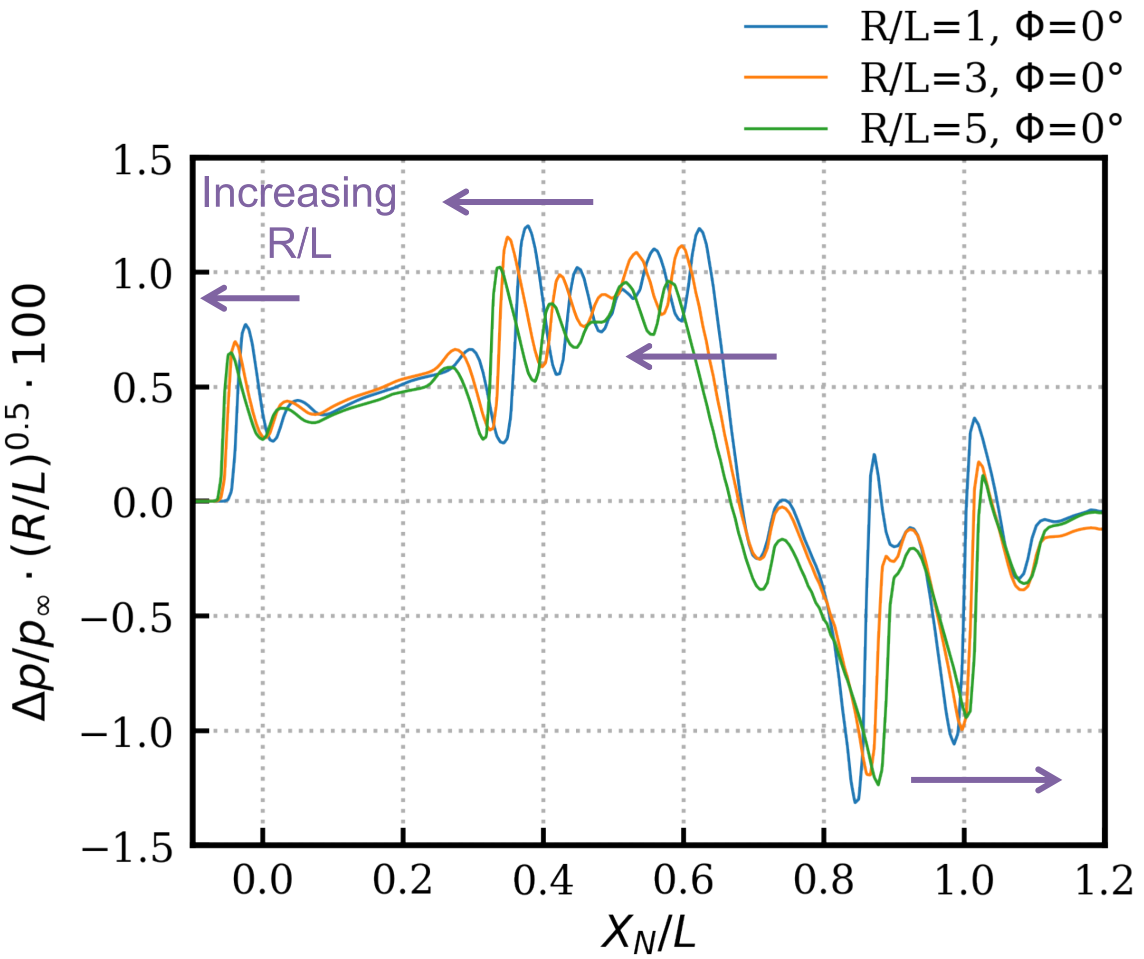

Increasing R/L

- positive pressure differences are propagating forward
- negative pressure differences are propagating rearward

grid: ws-mixed-100

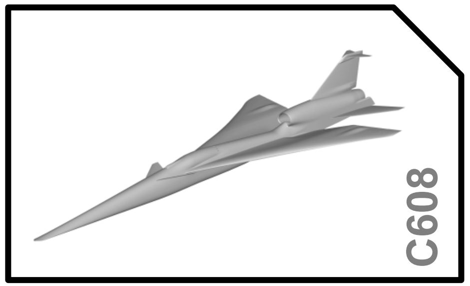

Results

C608 – Signature Propagation

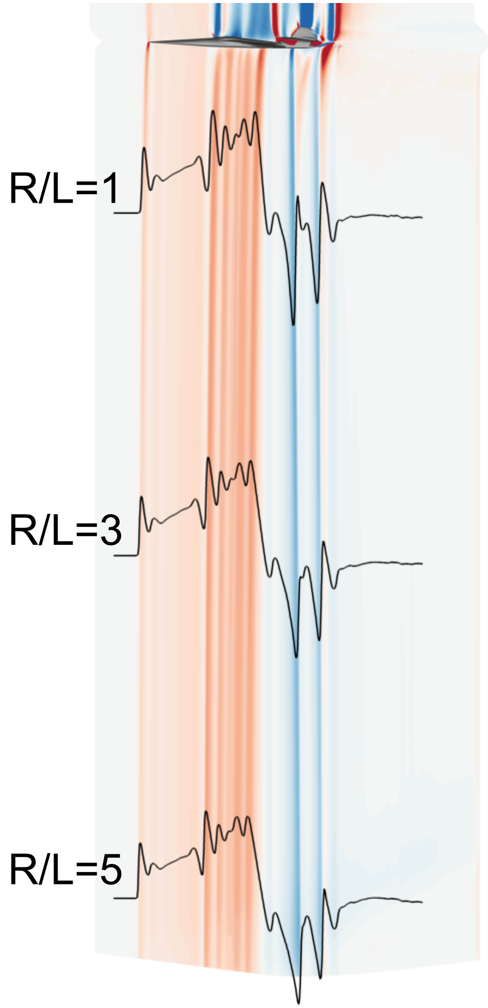

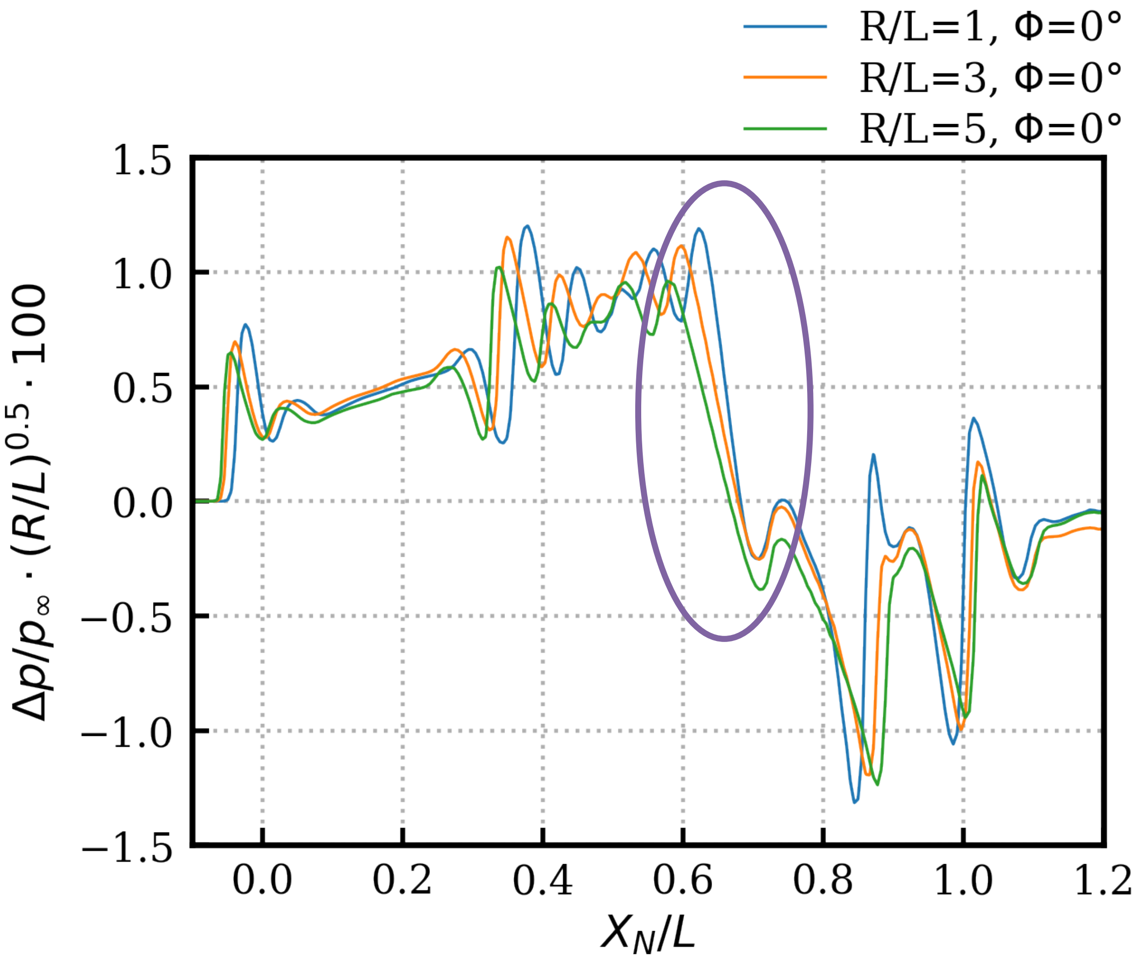

Increasing R/L

- positive pressure differences are propagating forward
- negative pressure differences are propagating rearward

→ gradient of the main expansion is decreasing

grid: ws-mixed-100

Results

C608 – Signature Propagation

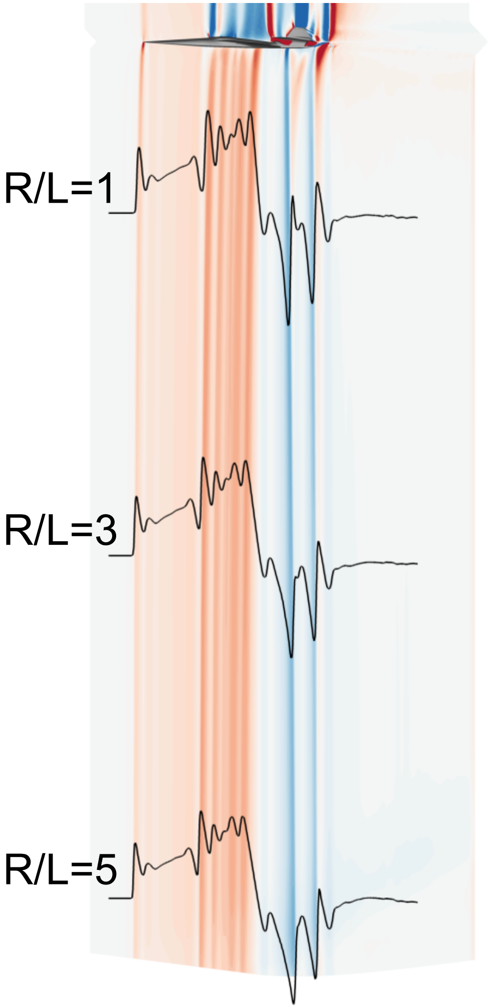

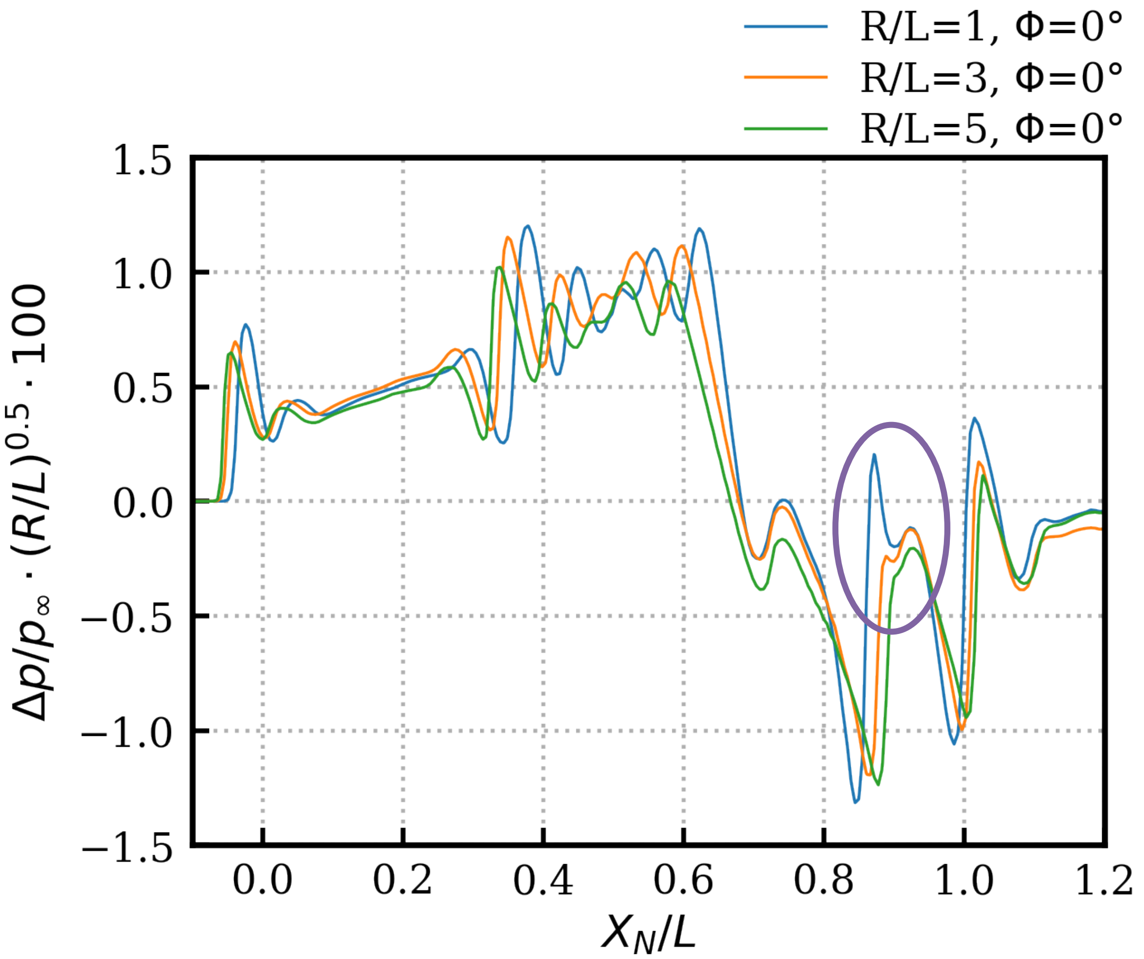

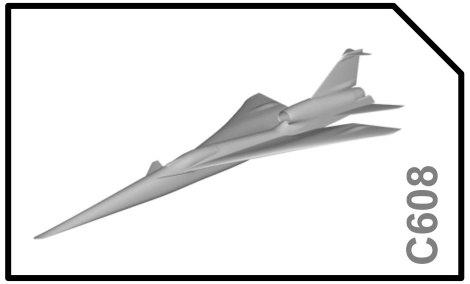

Increasing R/L

- positive pressure differences are propagating forward
- negative pressure differences are propagating rearward

→ gradient of the main expansion is decreasing

Pressure Signature at R/L=1

- Significant dissipation at the HTP leading edge shock

grid: ws-mixed-100

Results
C608 – Signature Propagation

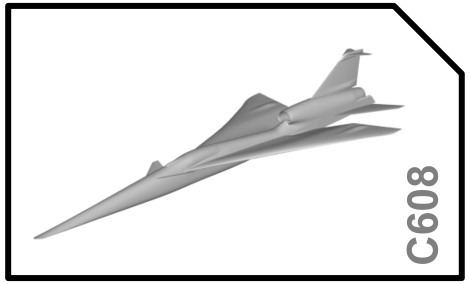

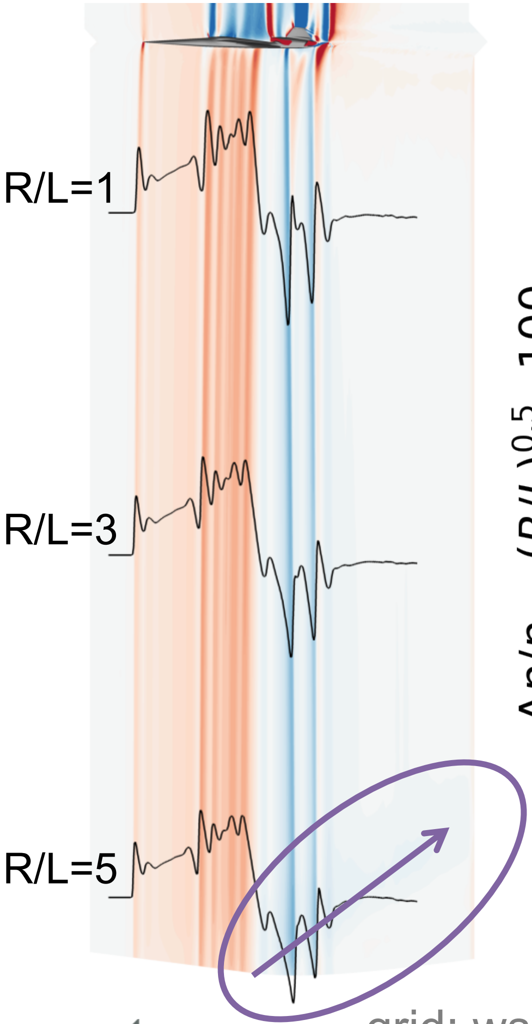

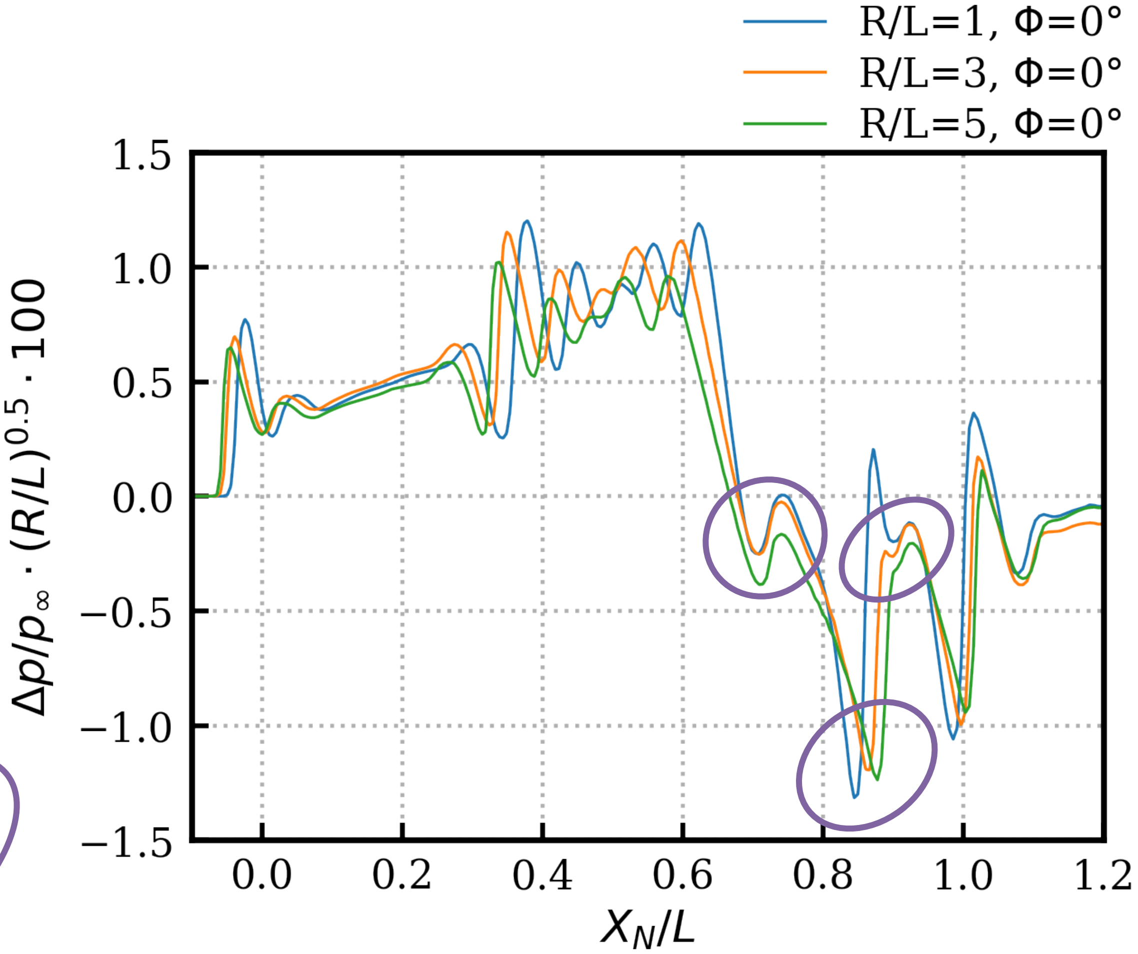

grid: ws-mixed-100

Increasing R/L

- positive pressure differences are propagating forward
- negative pressure differences are propagating rearward

→ gradient of the main expansion is decreasing

Pressure Signature at R/L=5

- unphysical reflections at the outer far-field boundary conditions

Results

C608 – Signature Convergence

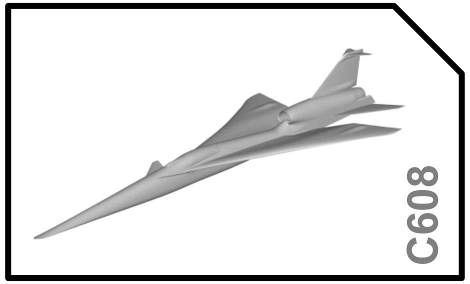

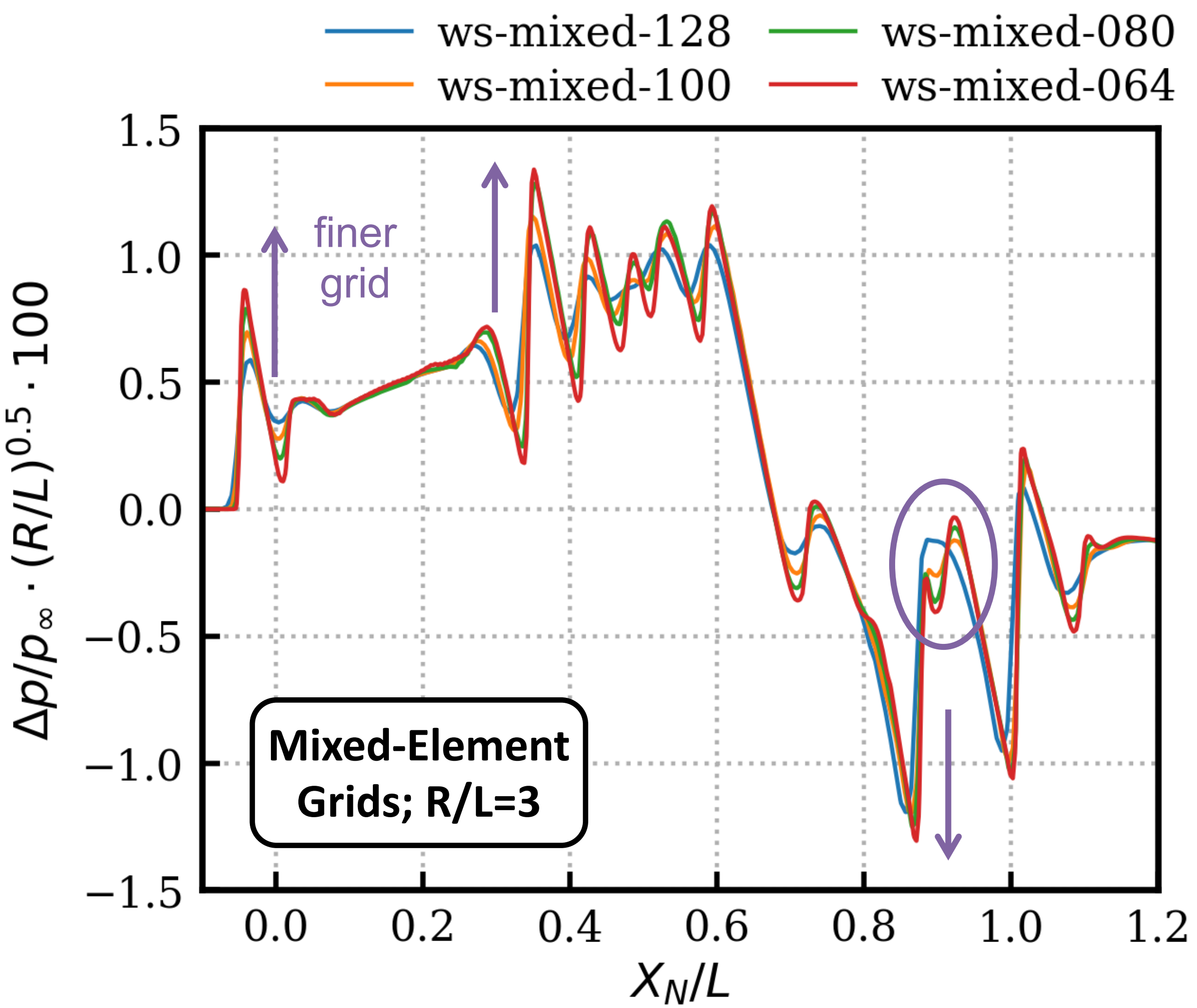

- magnitudes of compressions and expansions are larger for fine grids
- good signature convergence achieved for h ≤ 0.64
- most significant difference at the interaction of fuselage and HTP leading edge compression

  → no coalescence for fine grids

Results
C608 – Signature Convergence

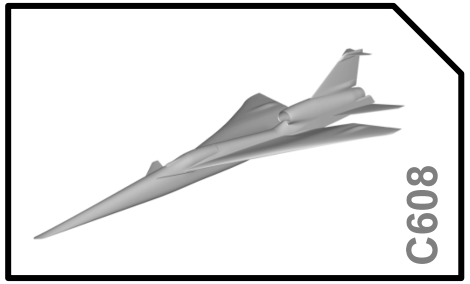

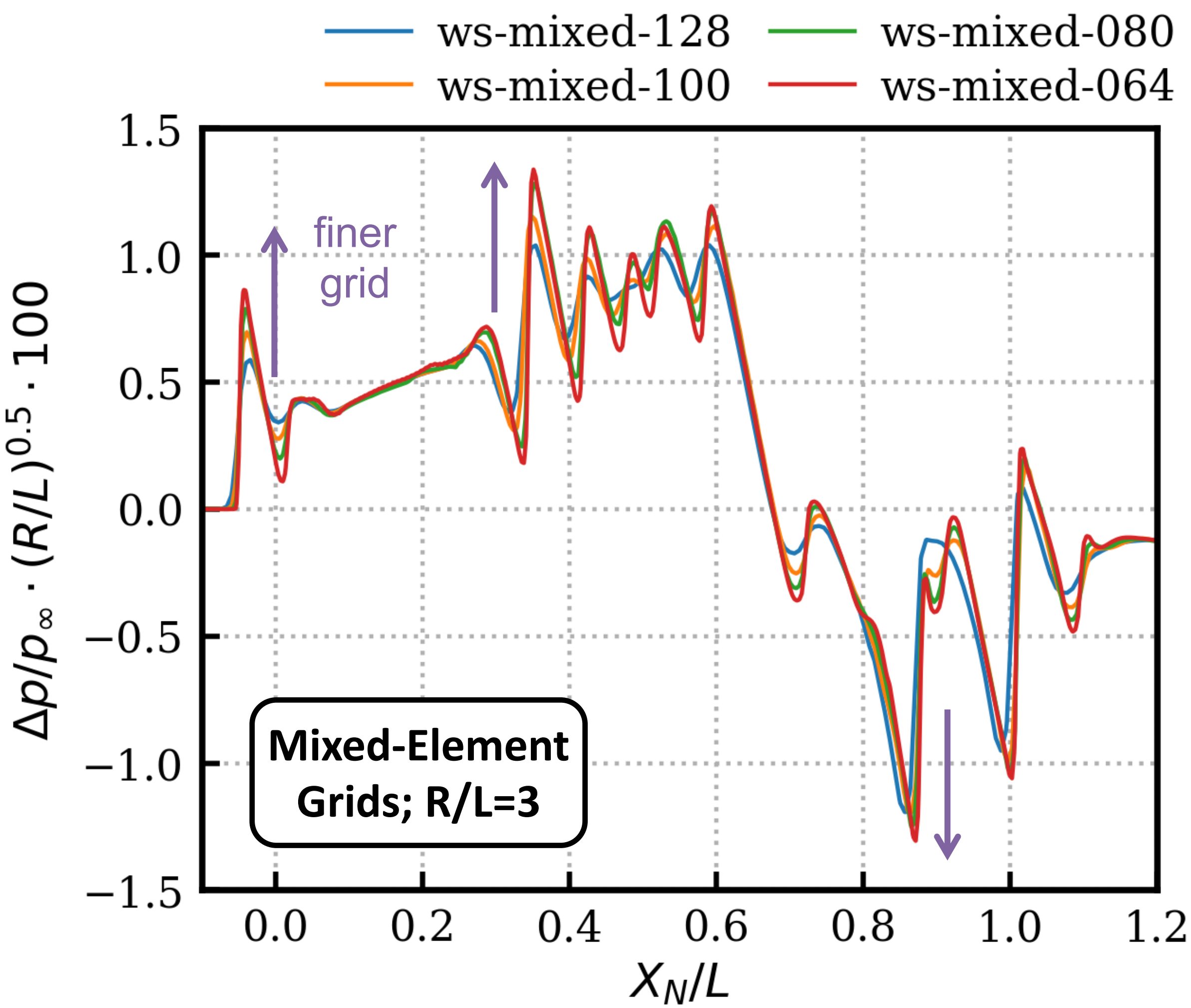

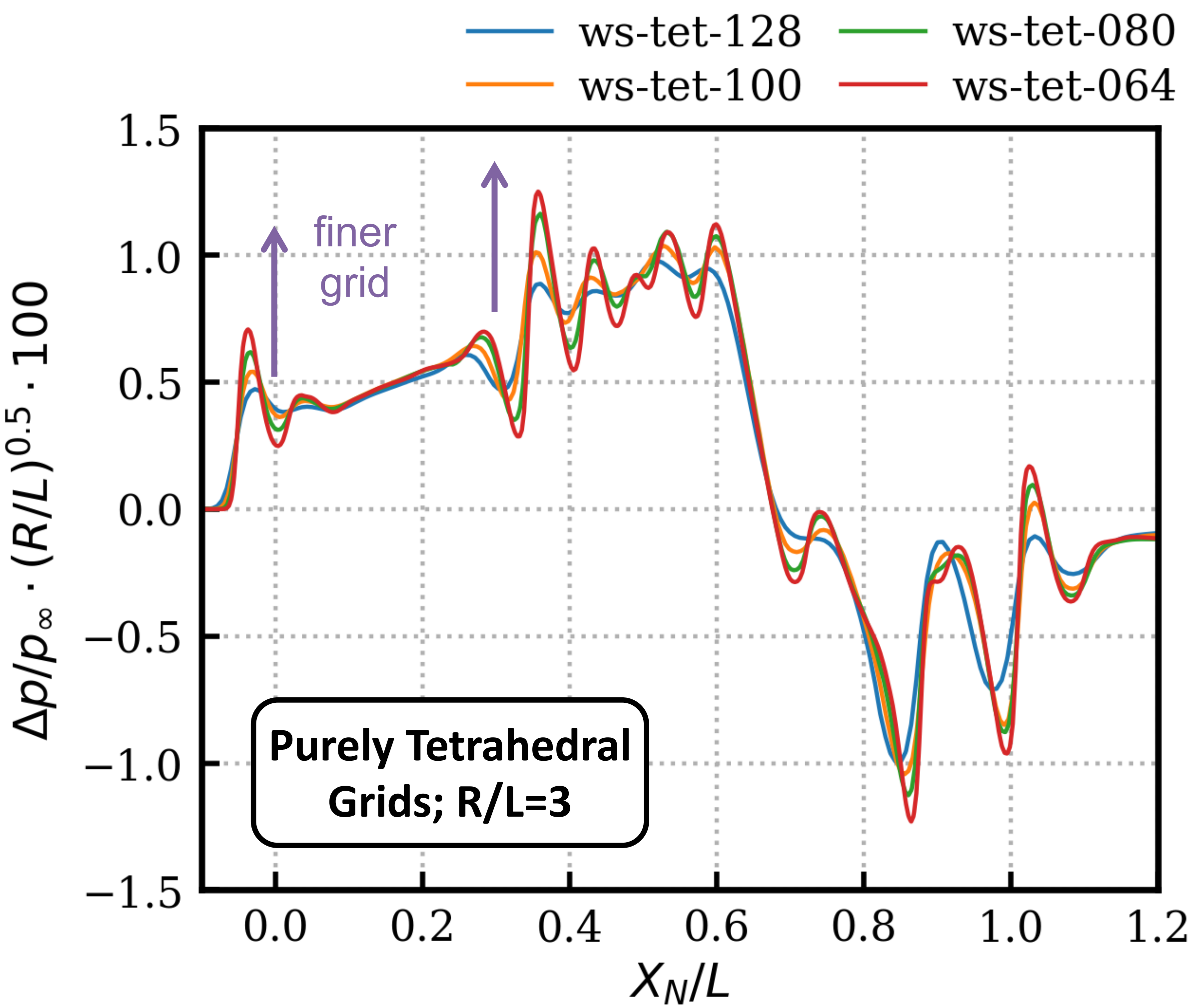

Results
C608 – Mixed vs Tet

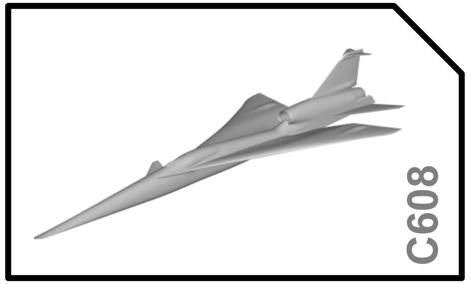

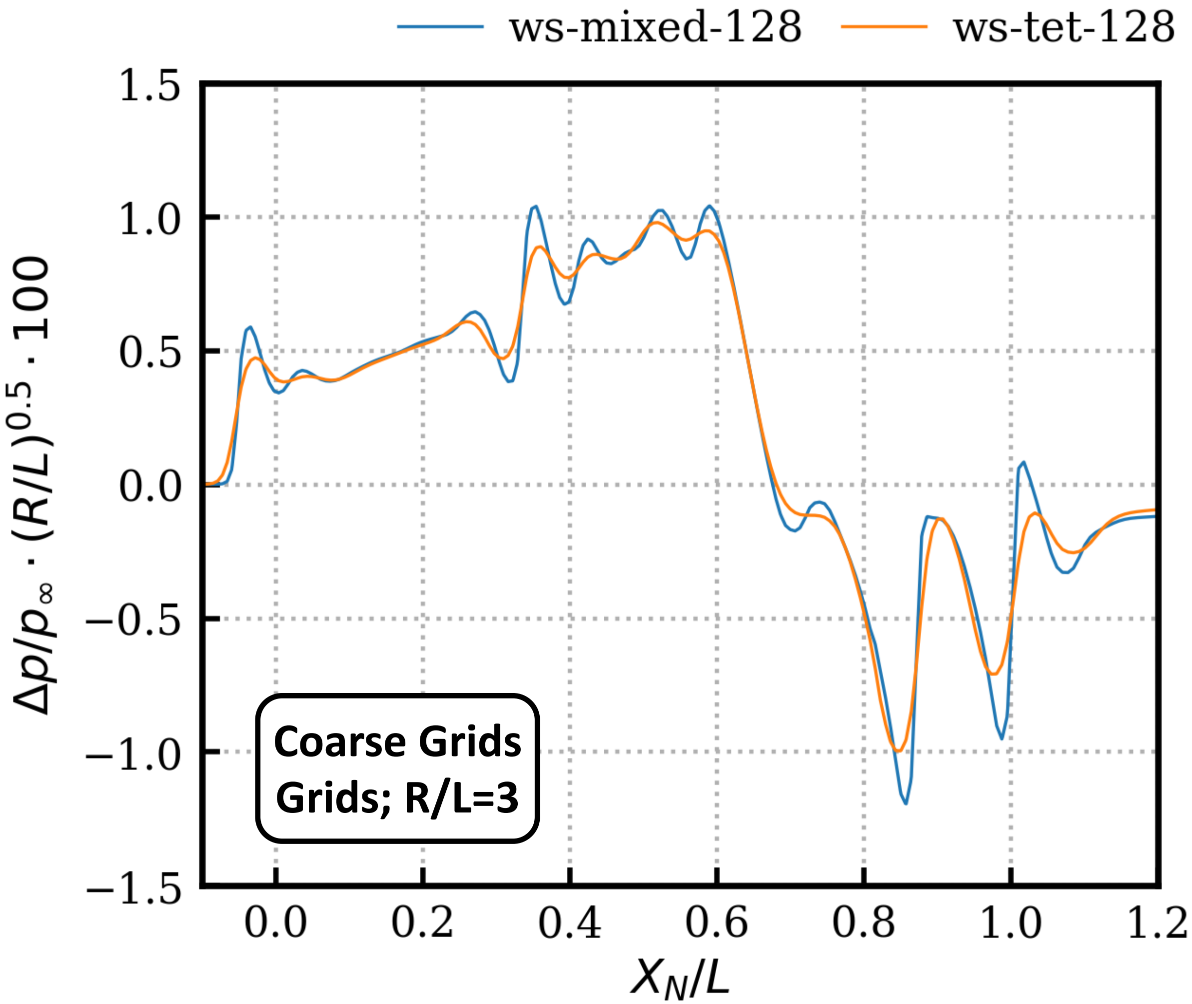

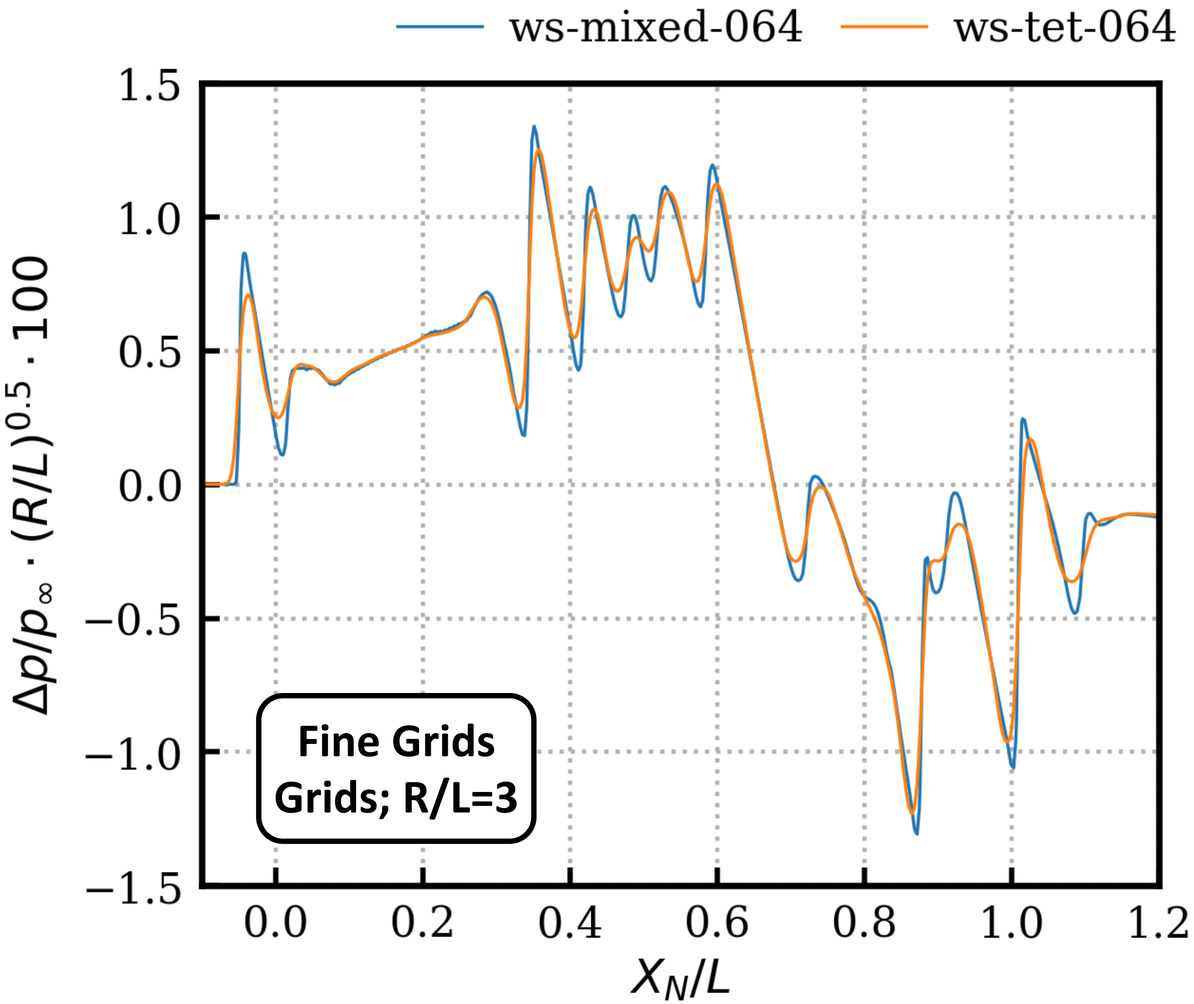

Summary / Highlights

Biconvex

- DLR TAU simulations with 6 workshop-provided and 5 CENTAUR-generated grids

- Biconvex on-track signature influenced by **surface resolution near symmetry plane**
- **Better resolution of the interaction with CENTAUR grids** compared to workshop-provided grids
- Nearly **no difference** between **mixed-element** and **purely tetrahedral** workshop-provided grids
- No signature convergence for workshop-provided grids but good signature convergence for CENTAUR grids

C608

- DLR TAU simulations with 11 workshop-provided grids

- **Good signature convergence** achieved for $h \leq 0.64$
- Most significant difference between refinement levels at the **HTP leading edge compression**
- Tetrahedral far-field is more dissipative than (semi-) structured far-field in TAU
- Radial extent of the far-field grid should be two body lengths larger than extracting distance to prevent influences of reflections

Outlook for Aviation Paper

Biconvex
- CENTAUR grid with structured block in interaction region
- CENTAUR grid with refined surface grid at symmetry plane

C608
- CENTAUR grids for the C608 case (Euler/RANS)
- Upload field data

Thank you!